KERNFORSCHUNGSZENTRUM

KARLSRUHE

Juli 1977 KFK 2493

Institut für Neutronenphysik und Reaktortechnik
Projekt Schneller Brüter

Calculational and Experimental Approaches to the Equation of State of Irradiated Fuel

M. Bober, W. Breitung, H. U. Karow, G. Schumacher

GESELLSCHAFT
FÜR
KERNFORSCHUNG M.B.H.

KARLSRUHE

GESELLSCHAFT FÜR KERNFORSCHUNG M. B. H.

KARLSRUHE

KERNFORSCHUNGSZENTRUM KARLSRUHE

KFK 2493

Institut für Neutronenphysik und Reaktortechnik
Projekt Schneller Brüter

CALCULATIONAL AND EXPERIMENTAL APPROACHES TO THE EQUATION OF STATE OF IRRADIATED FUEL*

M.Bober, W.Breitung, H.U.Karow, and G.Schumacher

*presented at IAEA Specialists' Meeting on "The Role of Fission Products in Whole Core Accidents", Harwell, UK, June 28th-July 1, 1977.

Gesellschaft für Kernforschung mbH., Karlsruhe

Abstract

The oxygen potential is an important parameter for the estimation of the vapor pressure of mixed oxide fuel and fission products. Dissolved fission products can have great influence on this potential in hypostoichiometric fuel. Therefore an attempt was made to calculate oxygen potentials of uranium-plutonium mixed oxides which contain fission products using models based on the equilibrium of oxygen defects. Vapor pressures have been calculated applying these data. The results of the calculation with various models differ especially at high temperatures above 4000 K.

Experimental work has been done to determine the vapor pressure of oxide fuel material at temperatures between 3000 K and 5000 K using laser beam heating. A measuring technique and a detailed evaluation model of laser evaporation measurements have been developed. The evaluation model describes the complex phenomena occurring during surface evaporation of liquid oxide fuel. Vapor pressure measurements with UO_2 have been carried out in the temperature region up to 4500 K. With thermodynamic calculations the required equilibrium vapor pressures (EOS) can be derived from the vapor pressures measured.

The caloric equation-of-state of the liquid-vapor equilibrium of the fuel up to temperatures of 5000 K has been considered theoretically.

Ansätze zur Berechnung und experimentellen Bestimmung der Zustandsgleichung von bestrahltem Brennstoff

Zusammenfassung

Das Sauerstoffpotential ist ein wichtiger Parameter für die Bestimmung des Dampfdrucks von Mischoxid-Brennstoff und Spaltprodukten. Gelöste Spaltprodukte können einen großen Einfluß auf dieses Potential in unterstöchiometrischem Brennstoff ausüben. Deshalb wurde versucht mit Modellen, die auf dem Gleichgewicht der Sauerstoffeffekte beruhen, das Sauerstoffpotential von Uran-Plutonium-Spaltprodukt-Mischoxiden zu ermitteln. Anhand dieser Daten wurden Dampfdrücke berechnet, deren Werte oberhalb 4000 K stark vom verwendeten Defektmodell abhängen.

Unter Anwendung von Laserheiztechniken wurde die Verdampfung von Oxidbrennstoff bei Temperaturen zwischen 3000 K und 5000 K experimentell untersucht. Hierzu wurden eine geeignete Meßtechnik und ein Auswertemodell entwickelt. Das Auswertemodell beschreibt die komplexen Vorgänge, die während der Oberflächenverdampfung von flüssigem Brennstoff ablaufen. An UO_2 wurden Dampfdruckmessungen im Temperaturbereich bis 4500 K durchgeführt. Mit Hilfe thermodynamischer Rechnungen lassen sich aus den Messungen die gesuchten Gleichgewichtsdampfdrücke ermitteln.

Die kalorische Zustandsgleichung des Flüssig-Dampf-Gleichgewichts des Brennstoffs wurde bis zu Temperaturen von 5000 K theoretisch untersucht.

1. INTRODUCTION

The gas pressure development in an irradiated mixed oxide fuel is mainly influenced by fission gases and volatile fission products in the temperatur region below the melting point and by the fuel material itself and the less volatile fission products in the temperature region above 4000 K [1].

Besides the temperature, the important factors for the vapor pressure are the oxygen potential of the fuel and the concentration of fission products in the fuel. As demonstrated by the calculations of Rand and Markin [2] the oxygen potential influences strongly the pressure of vapor species above (U Pu)O_2. The pressure of the species U, UO, UO_2, Pu, PuO, PuO_2 varies over a range of more than five orders of magnitude by variation of the oxygen potential at 2000 K. Similar effects were observed with oxides of the fission products. Fission products dissolved in mixed oxide fuel on the other hand can influence significantly the oxygen potential of the irradiated mixed oxide. This was demonstrated for example by Tetenbaum [3] with the system U-Nd-O. In the first paragraph of the paper an attempt is made to calculate oxygen potentials of mixed oxides containing dissolved fission products. The model used is based on the equilibrium of oxygen defects in the mixed oxide [4].

The chemical state and distribution of fission products are further conditions that should be considered in calculations of the local and overalls pressures and the behavior of the fuel. Fission products are transported during the irradiation period and collect at different positions within the fuel pin. This process can produce high local concentrations of fission products, thus enabling elements with low overall concentrations to reach their saturation pressure. The distribution of fission products and their behavior in irradiated mixed oxide fuel is described in the second paragraph.

The third paragraph deals with the calculation of vapor pressures that has been conducted using a model described by Breitung [5] for uranium-plutonium mixed oxides. This model is based on the law of mass action and provides vapor pressures as a function of temperature and oxygen potential under consideration of the vapor pressures of the fission pro-

zum Druck eingereicht am : 15.9.1977

ducts calculated by Gabelnick and Chasanov [1].

An experimental method for the determination of vapor pressure at high temperatures up to 5000 K is described in the fourth paragraph. The evaporation device is equipped with a laser-beam heating. Experiments with UO_2 show the applicability of the apparatus for the measurement of vapor pressures at high temperatures.

The last paragraph deals with the thermodynamic state and with the internal energy and enthalpy function of saturated fuel vapor at temperatures to 5000 K. These variables have been deduced by means of statistical mechanics from the molecular structure and from the kinetic and plasma state of UO_2.

2. OXYGEN POTENTIAL IN IRRADIATED MIXED OXIDE FUEL

2.1 Oxygen potential of $(U\ Pu)O_{2\pm x}$

The oxygen potential of the fuel determines the equilibrium between the condensed and all the gaseous species and thus the total vapor pressure. Therefore a pertinent selection of the numerous measured data is necessary.

The oxygen potential of $(U,Pu)O_{2\pm x}$ has been measured up to 2550 K, but the agreement of the different results is not good. Even at low temperatures (1300 K), measurements with identical (U,Pu)-mixed oxide specimens by two different laboratories gave $\Delta\bar{G}_{O_2}$-values which differ up to 5 kcal/mol [18]. To reduce these experimental discrepancies several semi-empirical models for $\Delta\bar{G}_{O_2}$ have been developed which can provide a basis for extrapolations to high temperatures. In these models, the oxygen partial pressures are described as a function of the temperature and the fuel composition by a set of equilibrium relations among postulated lattice defects. The equilibrium constants needed are evaluated from measured $\Delta\bar{G}_{O_2}$-data.

In Blackburn's model [9] the (U,Pu) mixed oxide contains U^{2+}, U^{4+}, U^{6+}, Pu^{2+}, Pu^{3+} and Pu^{4+} ions. Four equilibrium relations for these ions, and uranium-, plutonium- and oxygen conservation equations are used to calculate oxygen pressures as a function of fuel composition and temperature. In Fig.1 results are shown for several O/U+Pu ratios and temperatures which were obtained from this model [1,18] .

In the model of de Franceo and Gatesoupe [10] clusters of 8 metal atomes (U to Pu) are assumed. The Pu-clusters are proposed to have up to 4 oxygen vacancies, which give Pu valencies from 4.0 to 3.0. The U-clusters can have one or two oxygen vacancies or up to three oxygen interstititals, which give U valencies from 3.5 to 4.75. With these 11 cluster defects 9 equilibrium relationships can be formulated, the equilibrium constants of which were determined by a least square fitting procedure of $\Delta\bar{H}_{O_2}$ - and $\Delta\bar{G}_{O_2}$-measurements on PuO_{2-x}, UO_{2+x} and $(U,Pu)O_{2\pm x}$. For the purposes of this work, the system of equilibrium equations was solved with the given equilibrium constants up to 5000 K. Some results are shown in Fig.1.

For the sake of comparison Fig.1 contains also some data points from the model of Schmitz [7,19] for $(U,Pu)O_{2-x}$ and from the model of Breitung [4] for $(U,Pu)_{2\pm x}$. However, these models are not appropriate for extrapolation to very high temperatures because they include only Pu^{3+}, Pu^{4+}, U^{4+} [17] resp. Pu^{3+}, Pu^{4+}, U^{4+}, U^{5+} ions [4] and because the equilibrium constant were determined from small temperature ranges.

From Fig.1 the following conclusions can be drawn:

a) The oxygen potentials of hypo- and hyperstoichiometric (U,Pu) mixed oxides approach that of stoichiometric (U,Pu) mixed oxide with increasing temperature, that means, the O/M ratio will not have a great influence on the oxygen potential at high temperatures.
b) The extrapolation of the two quite different models [9] and [10] to high temperatures yields similar oxygen potentials up to 4200 K. Above 4200 K the agreement deteriorates.
c) From the envelope of all data points of the four models for $(U_{.80}Pu_{.20})O_{1.98}$ the uncertainty in $\Delta\bar{G}_{O_2}$ values is estimated to be about ±6 kcal/mol at low temperatures and ±12 kcal at 5000 K.

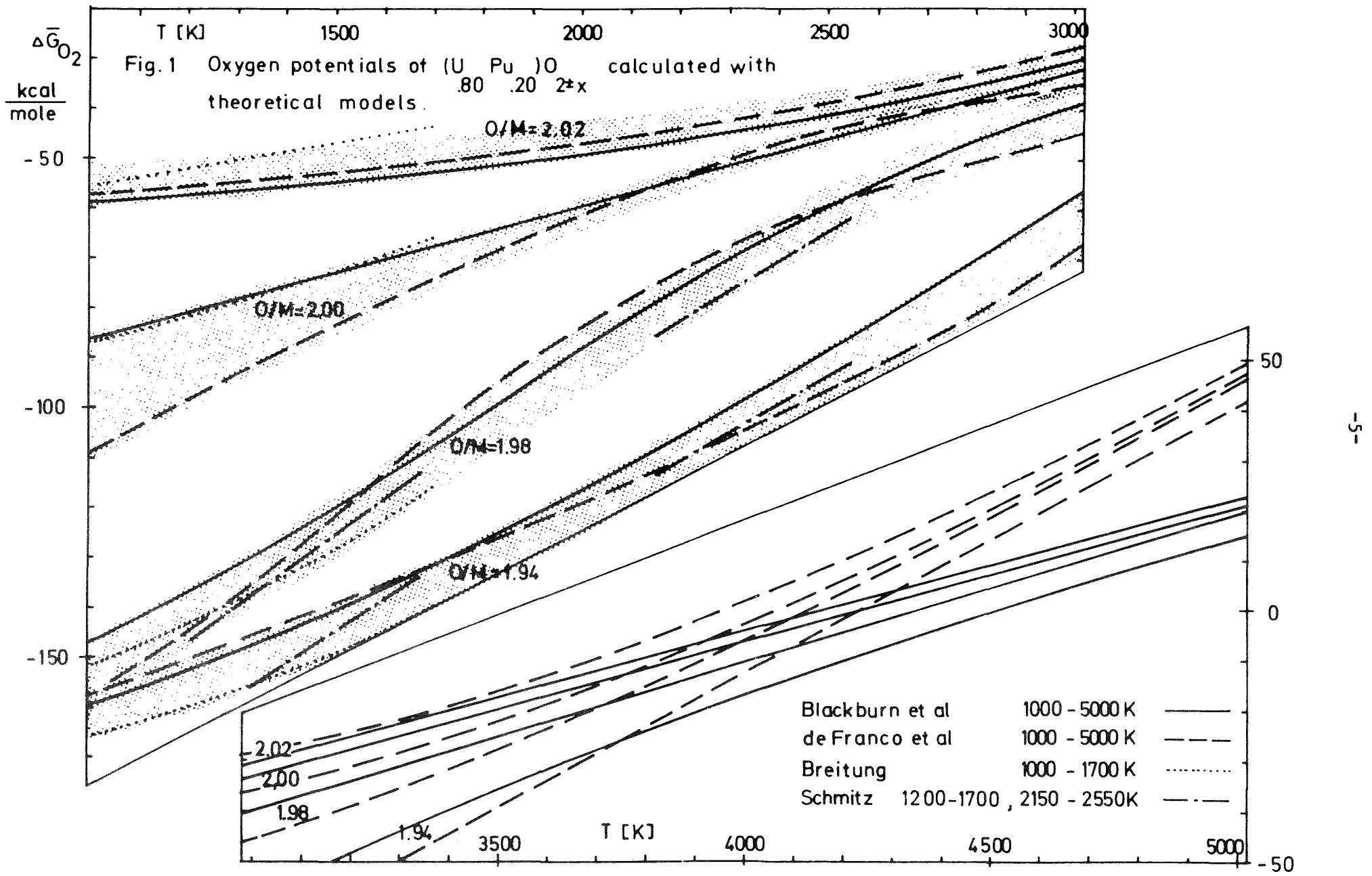

Fig. 1 Oxygen potentials of $(U_{.80}Pu_{.20})O_{2\pm x}$ calculated with theoretical models.

2.2 Oxygen potential of $(U,Pu)O_{2\pm x}$ with fission products

If one intends to calculate vapor pressures of irradiated $(U,Pu)O_2$ fuel the main problem that arises concerns the oxygen potential since no $\Delta\bar{G}_{O_2}$ measurements exist on irradiated fuel. The following chapter deals with the question how the oxygen potential of the U-Pu-O system is changed when fission products are added.

From the free enthalpies of formation and the yields of the fission products, Ce and Nd can be expected to have the greatest influence on the oxygen potential of $(U,Pu)O_2$ fuel. $\Delta\bar{G}_{O_2}$ measurements on (U,Ce) and (U,Nd) mixed oxides are used, to derive equilibrium relations between oxygen pressure, U-ions, Ce-ions and Nd-ions, respectively. With these relations, (U,Pu,Ce) and (U,Pu,Nd) mixed oxides will be modelled.

2.2.1 $(U_{1-z}Ce_z)O_{2-x}$ mixed oxides

The oxygen potential measurements of Markin, Crouch [20] on sub-stoichiometric (U,Ce) mixed oxides, can be interpreted in assuming that the uranium ions remain tetravalent and that Ce-ions are reduced from 4^+ to 3^+ according to the following reaction:

$$2Ce^{4+} + O^{2} \rightarrow Ce^{3+} + [\bar{C}e^{3+} \cdot V_o^{\cdot\cdot}] + \frac{1}{2} O_2 \qquad (1)$$

Eq.1 postulates that the removal of an oxygen lattice ion from the (U,Ce) mixed oxide is connected with the formation of one isolated Ce^{3+}-ion and one Ce^{3+}-ion bound to the oxygen vacancy. From Eq.1 follows with the mass action law and the appropriate molar fraction (z=fraction of cerium):

$$K = \frac{[Ce^{3+}]\,[Ce^{3+} \cdot V_o]\,p_{O_2}^{1/2}}{[Ce^{4+}]^2[O_o^2]} = \frac{x \cdot x \cdot p_{O_2}^{1/2}}{(z-2x)^2(2-x)}$$

or with $(2-x) \approx 2$ and $k' = 2\sqrt{2K}$

$$\log \frac{2x}{z-2x} = \log k' - \frac{1}{4} \log p_{O_2} \qquad (2)$$

According to Eq.2, a plot of $\log \frac{2x}{z-2x}$ versus the logarithmus of the measured oxygen pressure should give a line with the slope $-\frac{1}{4}$ independent of the Ce concentration z of the (U,Ce) mixed oxides. (The quotient $\frac{2x}{z-2x}$ is equal to the ratio of $[Ce^{3+}] / [Ce^{4+}]$ in the (U,Ce) mixed oxide)

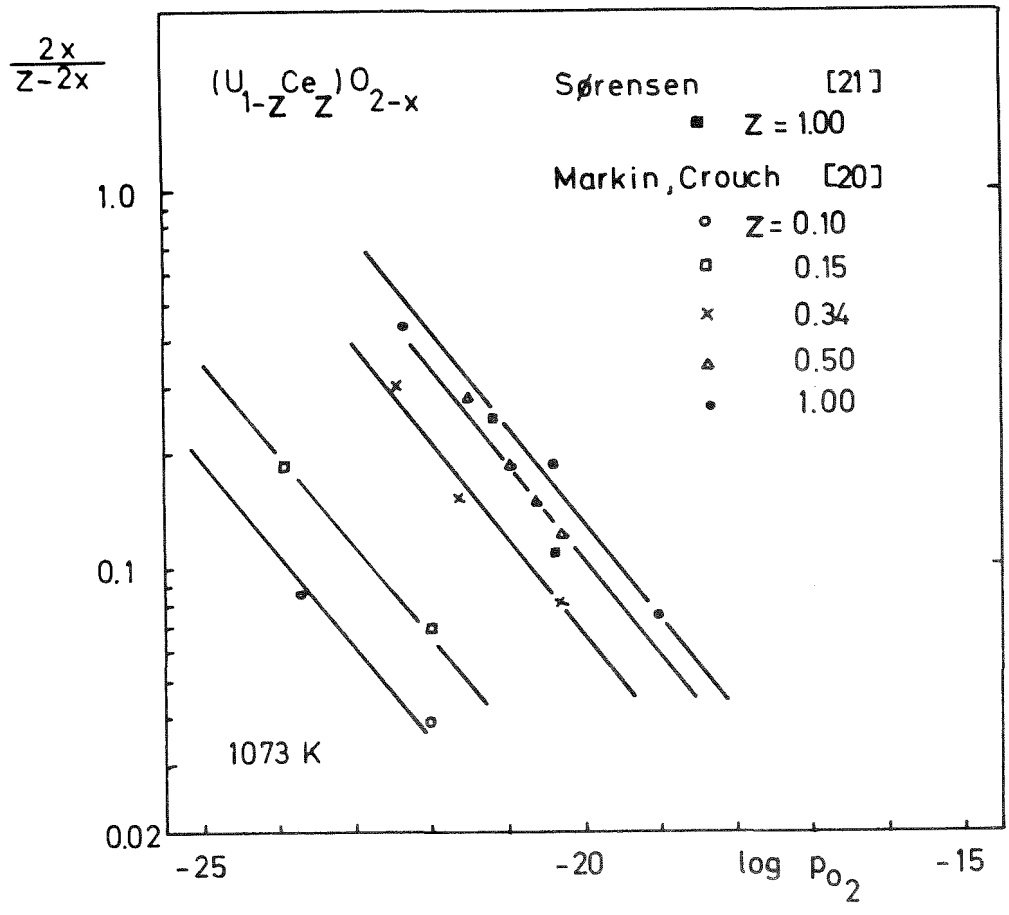

Fig.2 Measured oxygen potentials of $(U_{1-z}Ce_z)O_{2-x}$

Plotting the results of Markin, Crouch [20] and Sorensen [21] in this way, shows that the $\Delta\bar{G}_{O_2}$ data for mixed (U,Ce) oxides with high cer fractions ($z = 0.5...1.0$) can be represented by one line with the slope $-\frac{1}{4}$ (Fig.2) within the experimental uncertainties. From Fig.2 the equilibrium constant k' can be determined. Fig.2 shows that for cerium fractions less than about 0.5 the measured oxygen pressures yield lines which shift to smaller oxygen pressures with decreasing Ce content. This means that the Ce-ions in the (U,Ce) mixed oxides are increasingly stabilized against reduction (from Ce^{4+} to Ce^{3+}) with increasing U-content.

This behavior can be accounted for by introducing an empirial activity factor f into Eq.2:

$$\log f \cdot \frac{2x}{z-2x} = \log k' - \frac{1}{4} \log p_{O_2} \qquad (3)$$

f as determined from the shift of the lines in Fig.2 is shown in Fig.3.

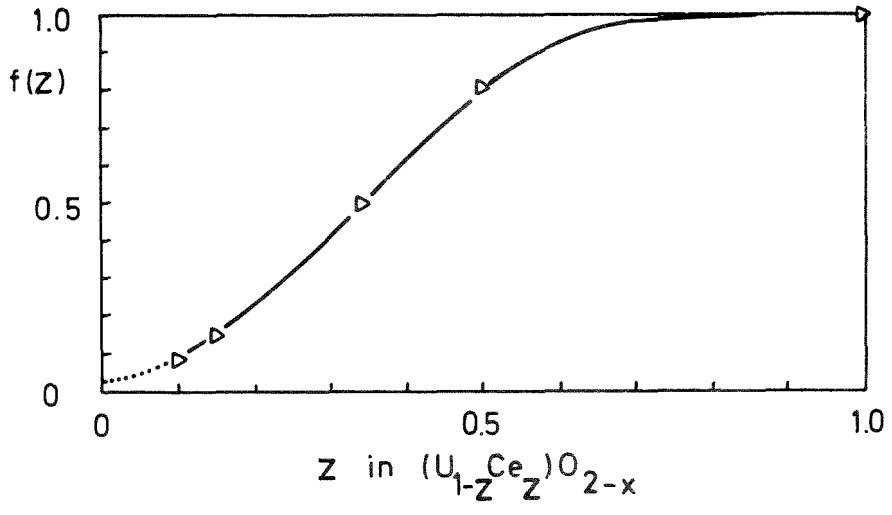

Fig.3 Empirical activity factor for Ce ions in $(U,Ce)O_{2-x}$

Eq.3 can be written as

$$\log f(z) + \log \frac{[\bar{Ce}^{3+}]}{[\bar{Ce}^{4+}]} = \log k' - \frac{1}{4} \log p_{O_2} \qquad (4)$$

Eq.4 describes the equilibrium between Ce^{3+}, Ce^{4+}-ions and the oxygen pressure in the presence of U-ions, which are assumed to be all tetravalent.

2.2.2. $(U_{1-y-z}Pu_yCe_z)O_{2-x}$ mixed oxides

In a similar investigation of (U,Pu) mixed oxides, for the equilibrium of Pu^{3+} and Pu^{4+} in the presence of U ions it was found [4]:

$$\log \frac{[\bar{Pu}^{3+}]}{[\bar{Pu}^{4+}]} = -8.2 - \frac{1}{4} \log p_{O_2} \qquad (5)$$

In [4] it was assumed that a substoichiometric (U,Pu) mixed oxide contains Pu^{3+}-, Pu^{4+}- and U^{4+}-ions.

Now (U,Pu,Ce) mixed oxides can be modelled by combining Eqs.4 and 5. This implies the additional assumption that the equilibrium in Eqs.4 and 5 are not changed very much if the two systems U-Pu-O and U-Ce-O are combined.

The conservation equations which must be fulfilled for the oxide $(U_{1-y-z}\ Pu_y\ Ce_z)O_{2-x}$ are:

$$[\bar{Ce}^{3+}] + [\bar{Ce}^{4+}] = z \qquad (6)$$

$$[\bar{Pu}^{3+}] + [\bar{Pu}^{4+}] = y \qquad (7)$$

$$3[\bar{Ce}^{3+}] + 4[\bar{Ce}^{4+}] + 3[\bar{Pu}^{3+}] + 4[\bar{Pu}^{4+}] = 2(2y+2z-x) \qquad (8)$$

The U ions are assumed to be tetravalent, therefore, the following oxygen fraction remains for the Ce- and Pu-ions:

$$(2-x) - 2(1-y-z) = 2y + (2z - x)$$

The equation system 4 to 8 has been solved for the oxygen pressure P_{O_2} for several Ce fractions z and oxygen deficiencies x. The resulting oxygen potentials are shown in Fig.4.

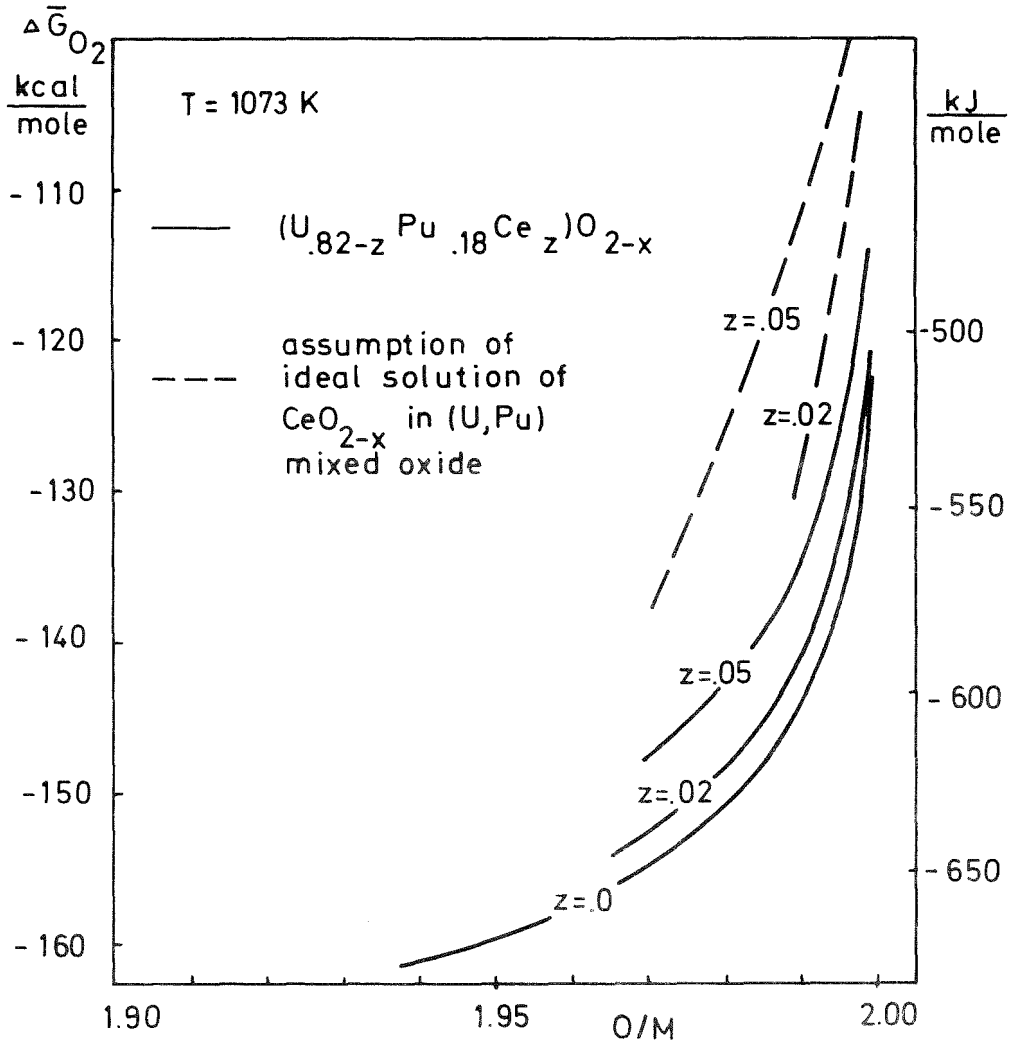

Fig.4 Oxygen potentials in $(U,Pu,Ce)O_{2-x}$

The following conclusions can be drawn from the model at 1073 K

a) At 1073 K the replacement of 2% uranium ions by cerium ions (≈ 10% burn up), raises the oxygen potential for 2-3 kcal/mole only.

b) If on the other hand, the equilibrium relation for pure cerium oxide (factor f=1 in Eq.4) is used, the oxygen potentials are 10 to 20 kcal higher than those of pure (U,Pu) mixed oxides. This shows that the assumption of $(U,Pu,Ce)O_{2-x}$ beeing an ideal solution of CeO_{2-x_1} in $(U,Pu)O_{2-x_2}$ is not justified (cf. Fig.4).

2.2.3 $(U_{1-z}\ Nd_z)O_{2-x}$ mixed oxides

The oxygen potential measurements of Tetenbaum [3] with (U,Nd) mixed oxides at 2550 K have been analysed in the same way as those of the (U,Ce) mixed oxides.

As Fig.5 shows, the points for (U.Nd) oxides with 10 and 20% Nd fall on one line, within the experimental uncertainties (±3 kcal in $\Delta\bar{G}_{O_2}$, i.e., ± 0.005 in x). At this high temperature the slope has changed to about -1/2,6.

2.2.4 $(U_{1-y-z}Pu_yNd_z)O_{2-x}$ mixed oxides

From Fig.5, which also shows the appropriate plots for UO_{2-x} and $(U,Pu)O_{2-x}$ at 2250 K, it can be seen that $(U,Pu)O_2$ is easier to reduce than $(U,\ Nd)O_2$ and this one again easier than UO_2. Therefore it can be anticipated that the introduction of Nd into (U,Pu) mixed oxide, will lower the oxygen potential. This indeed results from the model, as is shown in Fig.6. According to the calculations the oxygen potential of $(U_{.80}Pu_{.18}Nd_{.02})O_{2-x}$ is 1-2 kcal/mol lower than that of $(U_{.80}Pu_{.20})O_{2-x}$ at 2250 K.

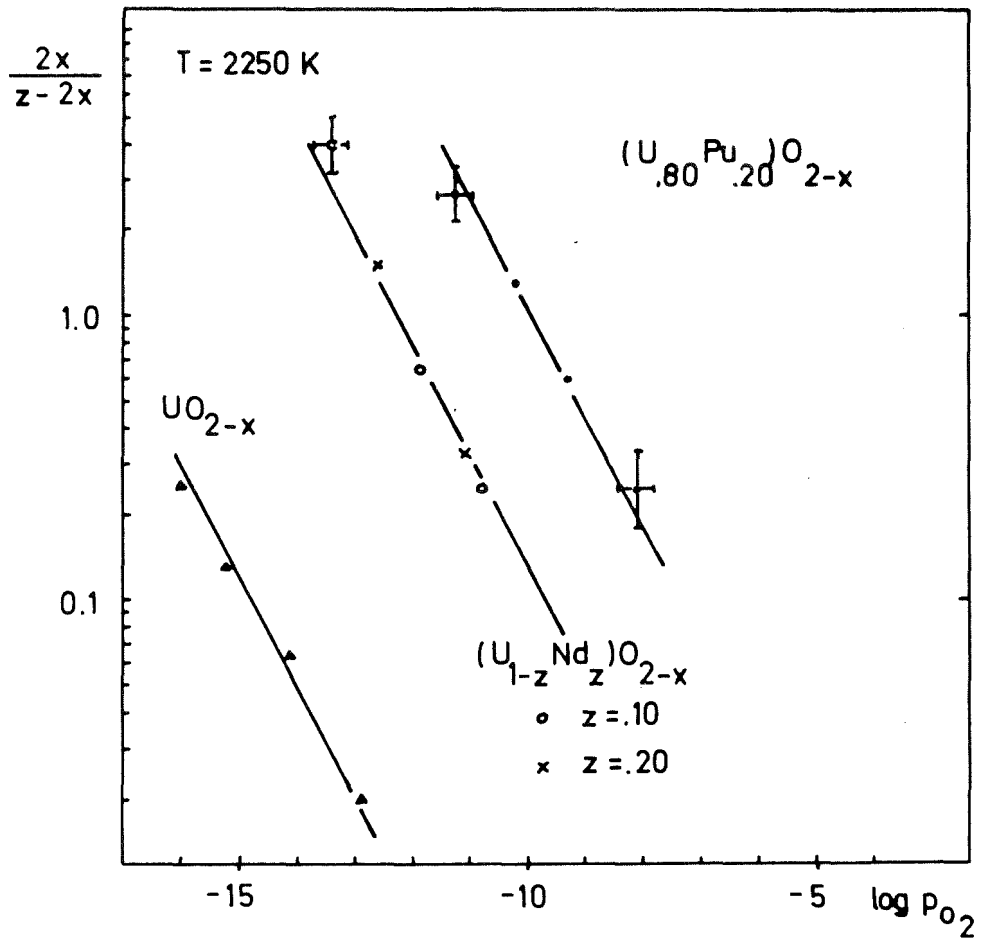

Fig.5 Oxygen potential in $(U,Nd)O_{2-x}$ compared with that of UO_{2-x} and $(U,Pu)O_{2-x}$ at 2250 K.

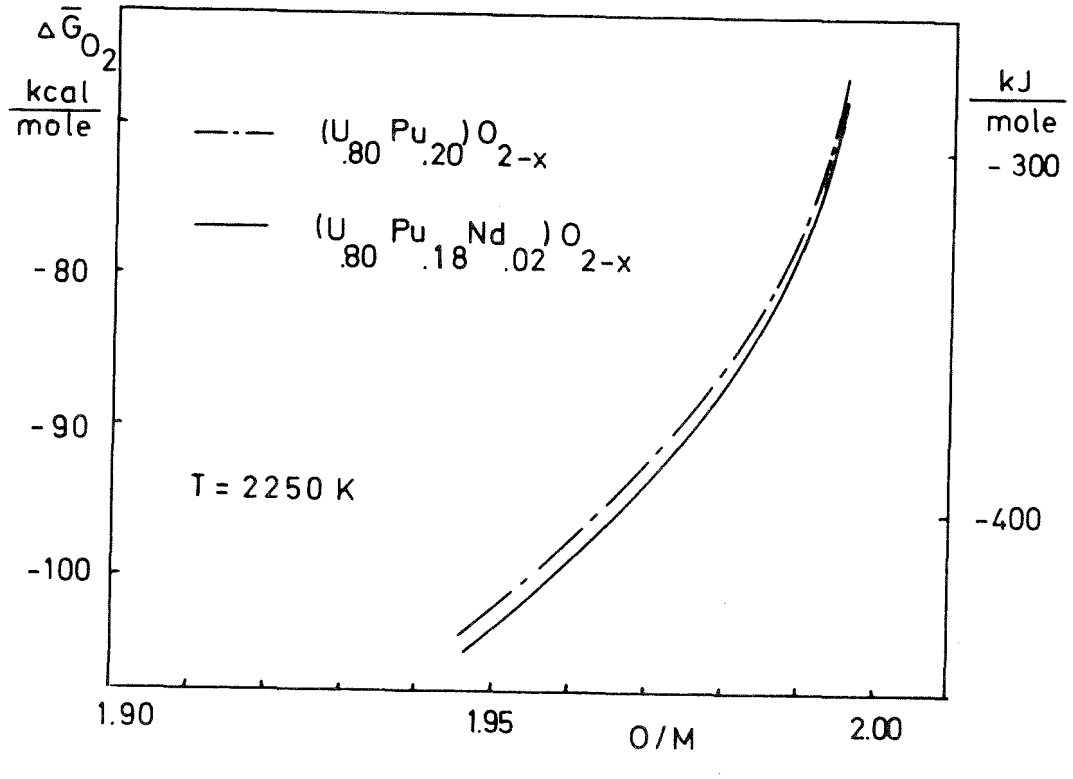

Fig.6 Oxygen potential in $(U,Pu,Nd)O_{2-x}$

2.2.5 Influence of fission products on the oxygen potential of $(U,Pu)O_{2\pm x}$

It was expected that the fission products Ce and Nd could have the greatest influence on the oxygen potential of the fuel, compared with the other fission products.

The result of the given estimation is, that Ce and Nd alter the $\Delta\bar{G}_{O_2}$ of the fuel only for some kcal/mole and that their influence is in opposite directions.

For these reasons the oxygen potential of irradiated fuel is assumed to be equal to that of pure $(U,Pu)O_2$ fuel.

2.3 Oxygen distribution in irradiated fuel

In the steep radial temperature gradient of a fuel pin under irradiation thermodynamic forces exist which transport oxygen to the rim of the fuel in hypostoichiometric fuel and to the center in hyperstoichiometric fuel. Thus the oxygen concentration varies with fuel radius and influences the local vapor pressure during the lifetime of the fuel pin

The oxygen distribution has been calculated for several overal Pu valencies in mixed oxide fuels with a thermal diffusion model by Sari and Schumacher [11] and estimated by Kleykamp [12] in irradiated fuel taking into account the Mo and MoO_2 concentrations measured in metallic and ceramic inclusions. Fig.7 shows the results. Dashed lines represent estimated and full lines calculated oxygen distributions.

A considerable deviation from the overall O/M can be observed at the rim (r/R=1) and at the center of the fuel pin that leads to marked differences in the oxygen potential. The real oxygen potentials produced by oxygen redistribution at the rim and in the center differ by up to 200 kJ/mol from that corresponding to an uniform oxygen distribution with O/M=1.976 (v_{Pu}=3.84) in $(U_{.70}Pu_{.30})O_{2-x}$. This gives a difference in oxygen partial pressure of about 4 orders of magnitude. Not so large are the deviations in hyperstoichiometric fuels in which the O/M in the center does not exceed 2.003 ($v_U \simeq 4.008$) due to the stabilizing effect of Mo.

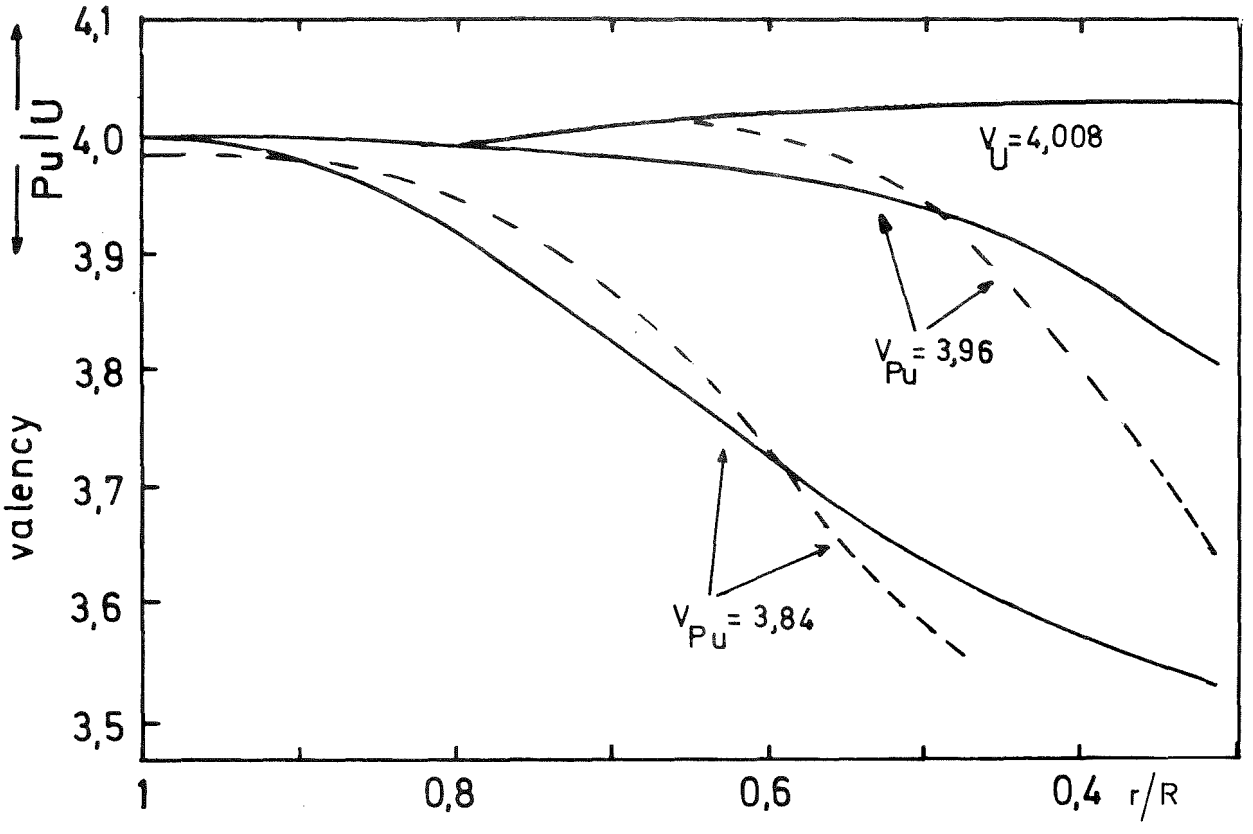

Fig.7 Calculated (full) and measured (dashed) U and Pu valencies along the radius of a $(U_{.80}Pu_{.30})O_{2\pm x}$ pin. $\bar{V}_{Pu}$ and $\bar{V}_U$ are the overall Pu- and U-valencies, respectively.

3. BEHAVIOR OF FISSION PRODUCTS AND ACTINIDES IN A FUEL PIN

The fission products in a burnt fuel pin can be divided in 3 groups with respect to their contributions to the pressure within the fuel:

1) Those which are in a condensed state throughout the fuel under normal operation conditions
b) Those which are volatile or in a condensed state depending on their position in the pin (temperature and oxygen potential)
c) Those which are always in the gaseous state.

Table 1 shows how the important fission products can be attached to the three divisions described. Fission products with yields lower than 0.5 cannot contribute essentially to the total vapor pressure at high temperatures. As shown by Gabelnick and Chasanov [1] vapor pressures of the principal contributors at 5000 K are in the order of 100 bar.

division	Oxides		Elements
	dissolved	precip.	
a	Ce, Eu, La, Nd, Pr, Pm, Sm, Gd Y, Zr, Nb	Ba, Zr, Ce, Sr	Mo Rh, Rb, Ru, Tc
b		Mo, Cs Tc, Te, Sn	Cs, J, Te, Cd, Pd As, Sn
c			Kr, Xe, J

The underlined Oxides are stable in hyperstoichiometric mixed oxide only

Table 1 Fission product elements and compounds in a burnt mixed oxide fuel with yields >0.5

Similar to oxygen the fission products are not uniformly distributed throughout the fuel pin. They are subjected to transport processes due to thermal diffusion and evaporation condensation [13]. Kleykamp [14,15] examined burnt oxide fuel of a fast reactor and described the distribution of the main fission products in metallic and ceramic inclusions. Pd, Cs, Te and Sn were found to be enriched at the fuel rim and in the gap while other fission products in inclusions are roughly at the same concentration throughout the fuel. This is in accordance with an out of pile investigation of metallic Ru-Mo inclusions in mixed oxide fuel under a temperature gradient [16]. It has been observed that those inclusions grow up to a limited size of 5-10 µm and become practically immobile in the fuel. In hyperstoichiometric fuel molybdenum is oxidized and migrates towards lower temperatures or collects in ceramic inclusions [15]. Both typs of inclusions will not be dissolved in liquid fuel but swept out in periods larger than the transition phase.

Dissolved fission products oxides are known to migrate to the center by thermal diffusion and towards lower temperatures by evaporation condensation processes with the exception of ZrO_2 which has a lower vapor pressure than UO_2 [13].

With the known investigations of fission product distributions a listing of fission product locations can be made as shown in Tab.2. In the case of Cs an enhanced accumulation can be observed in the border between fissile and fertile fuel.

about uniform distributed	Ru, Mo*, Rh, Tc, Sr, Pr
accumulation	
a) center	Zr, Nd, Nb
b) col-grains	Ce, (La), (Pm), (Sm), (Y)
c) unrestructured zone	Cs**, Mo**, Pd, Te, Tc**
d) gap	Cs, Te, Pd, Cd, J, As

* hypostoichiometric fuel

** hyperstoichiometric fuel

Table 2 Main location of fission products in mixed oxide fuel pins

Another important irradiation effect is redistribution of uranium and plutonium by thermal diffusion and evaporation-condensation [13]. In mixed oxide fuels with O/M ratios (Pu-valencies) relevant for fast breeder fuels it occurs always an accumulation of plutonium in the center of a fuel pin which ranges from 115 to 160% related to the initial concentration of plutonium. The accumulation of plutonium in the center as a function of the plutonium valency is depicted in Fig.8 [17] which contains the results of the known post irradiation examinations of fast breeder oxide fuels. A model recently developed by Breitung [36] taking in account thermal diffusion [13] and evaporation-condensation processes in migrating pores allows a prediction of redistribution of uranium and plutonium as well as of fission products if the necessary data are known.

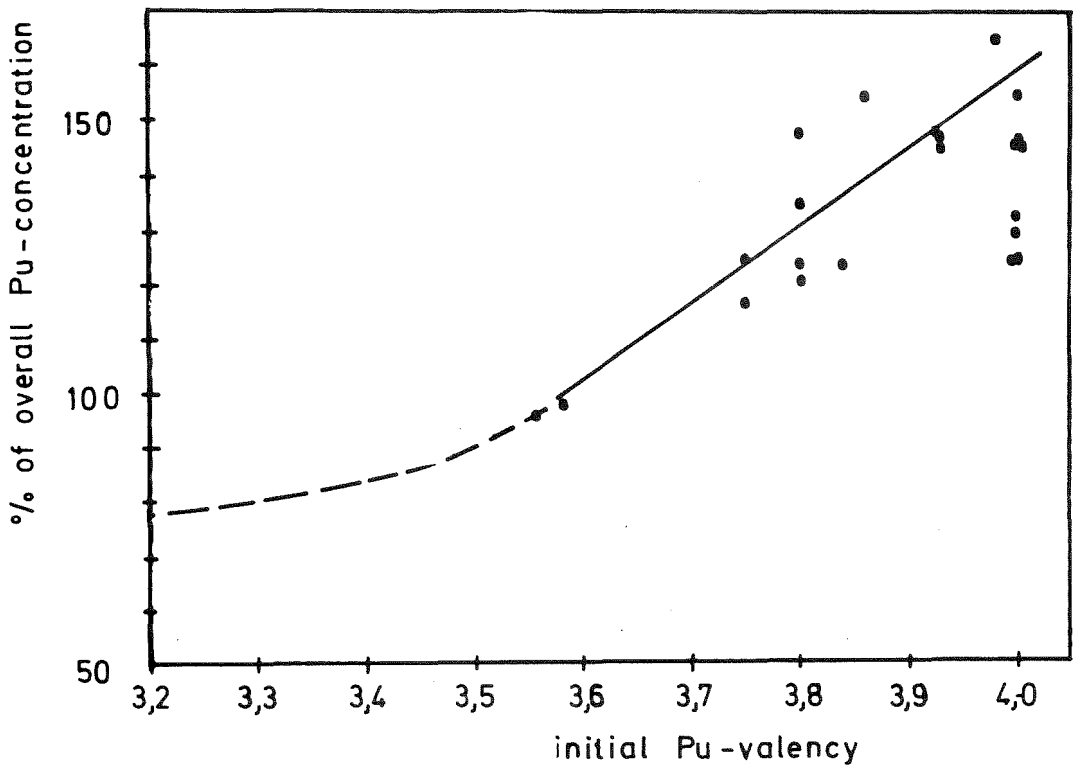

Fig.8 Pu-concentration at the central void as a function of the initial Pu-valence in irradiated fuel pins.

4. CALCULATION OF THE VAPOR PRESSURE OF IRRADIATED FUEL AT HIGH TEMPERATURES

The equilibrium vapor pressure of gaseous species $MO_B(g)$ evaporating from a solid or liquid metal oxide $MO_A(cond.)$ can be calculated from the evaporation reaction [2]:

$$MO_A(cond.) + \frac{B + A}{2} O_2(g) \rightarrow MO_B(g). \qquad (9)$$

This reaction includes also the evaporation of pure metals (A=B=0). For thermodynamic equilibrium the mass action law gives

$$\Delta G_{f,T}(MO_B) - \Delta G_{f,T}(MO_A) + RT \ln - \frac{p_{MO_B}}{a_{MO_A} \cdot p_{O_2}^{(B-A)/2}} = 0$$

or with $RT \ln p_{O_2} = \Delta\bar{G}_{O_2}$

$$\log p_{MO_B} = \log a_{MO_A} + \frac{\Delta G_{f,T}(MO_A) - \Delta G_{f,T}(MO_B) + \frac{B-A}{2}\Delta\bar{G}_{O_2}}{RT \ln 10} \qquad (10)$$

where the symbols have the following measurings:

p_{MO_B} = vapor pressure of the gaseous metal oxide MO_B.

a_{MO_A} = activity of the (evaporating) condensed oxide MO_A.

$\Delta G_{f,T}(MO_A)$ = free enthalpy of formation of the condensed oxide MO_A at temperature T,

$\Delta G_{f,T}(MO_B)$ = free enthalpy of formation of the gaseous oxide MO_B at temperature T

$\Delta\bar{G}_{O_2}$ = oxygen potential of the oxide system.

If the thermodynamic quantities on the right side of Eq.(10) are known, the vapor pressure of the gaseous specie MO_B can be calculated.

The total vapor pressure of pure $(U_{.80}\ Pu_{.20})O_{1.98}$ fuel was calculated according Eq.10 with both sets of oxygen potentials. For the free energies of formation the values given in [5] were used. The activity of uranium- and plutonium oxide was taken equal to their molar fraction. The difference in the results of both calculations is significant at temperatures above 4500°C as shown in Fig.9.

Calculations of fission product vapor pressures have been carried out by Gabelnick and Chasanov in a very careful and complete work [1]. They used the oxygen potential of pure $(U,Pu)O_2$ fuel [9], which seems to be justified by chapter 2. Since it is thought that the results of Gabelnick and Chasanov are the best estimate of fission product vapor pressures, at present possible, the calculation of fission product vapor pressures was not repeated. To estimate the total vapor pressure of irradiated (U,Pu) mixed oxide fuel we simply added their fission product vapor pressures to our calculated fuel vapor pressure, corrected for the altered activity of uranium and plutonium. The fission gas rentention is assumed to be 100% for this estimation.

The resulting total vapor pressure versus temperature curve of irradiated $(U_{.80}\ Pu_{.20})O_{1.98}$ fuel is shown in Fig.10 for several burnups. The calculations of fission product vapor pressures [1] were carried out

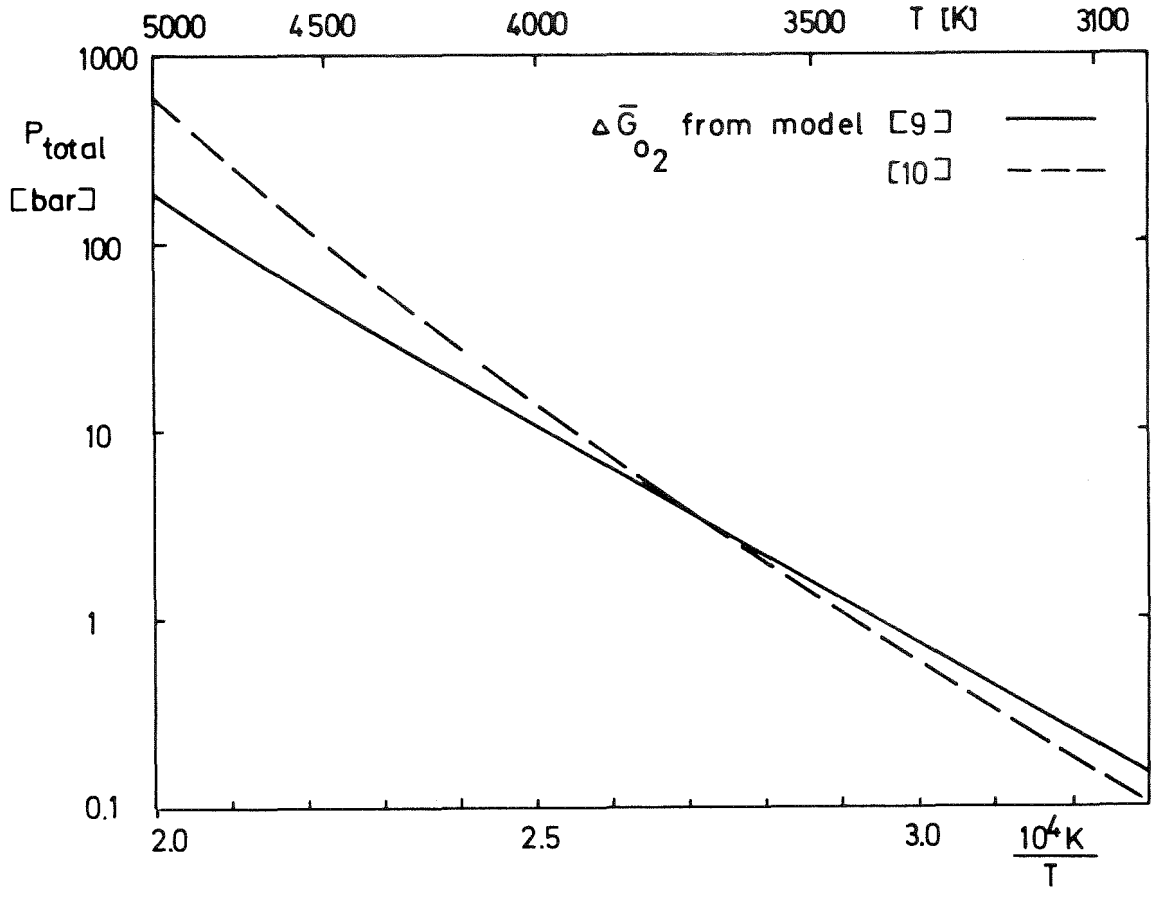

Fig.9 Total vapor pressure over mixed oxide calculated with two models for the oxygen potential.

with a fuel smear density of 5 g/cm^3, which is typical for a voided fast breeder reactor core.

Fig.11 shows the contributions of the gaseous species over mixed oxide fuel after 1% burnup to the total vapor pressure. Fission gases and volatile fission products (alkali metals) give the main contributions at low temperatures. Gaseous species of the fuel and of less volatile fission products become significant at temperatures above 4000 K. The vapor pressure of the fuel is taken from the full line in Fig.10. With the second model for the oxygen potential (dashed line in Fig.10) a much higher contribution of the fuel vapor is to be expected.

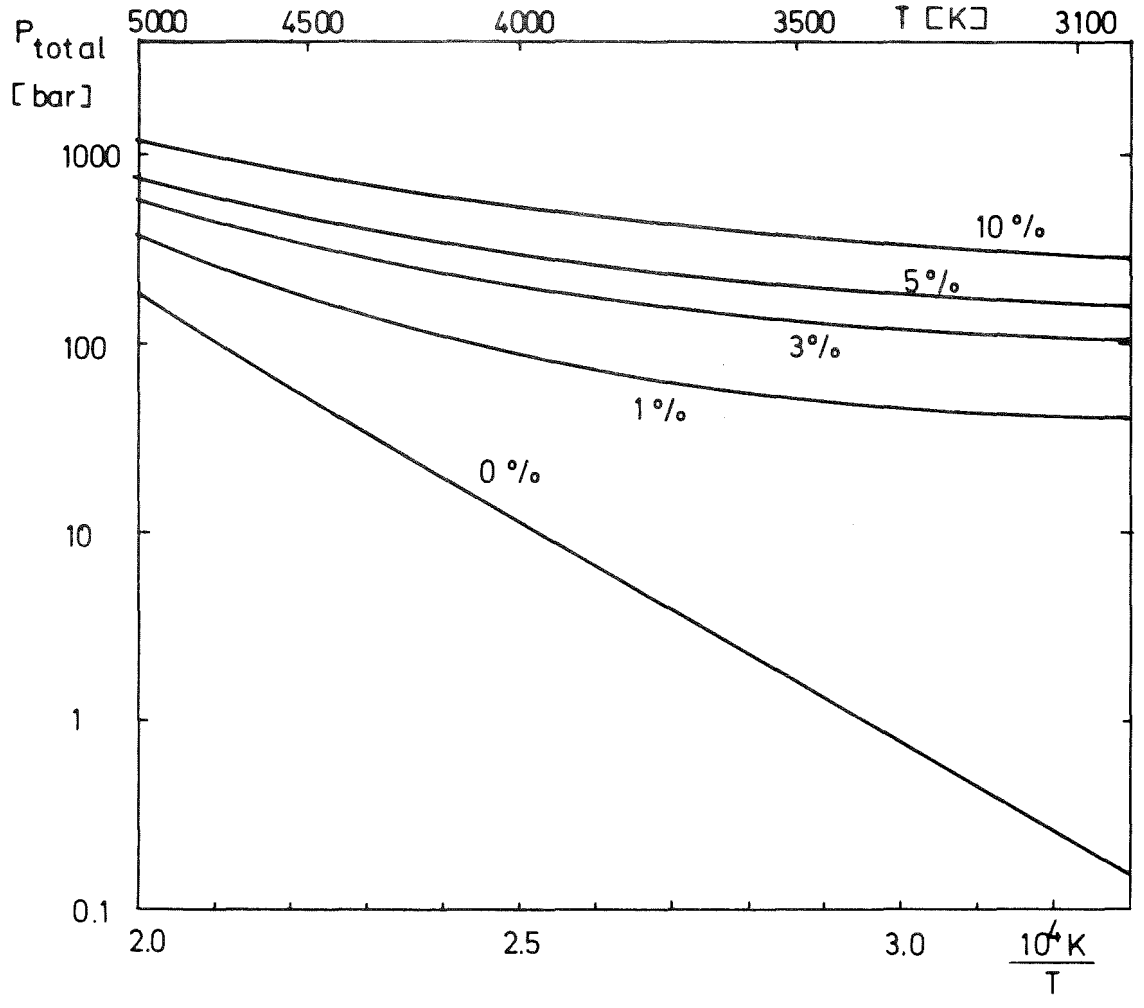

Fig.10 Pressure over burnt fuel. Parameter is the burnup.

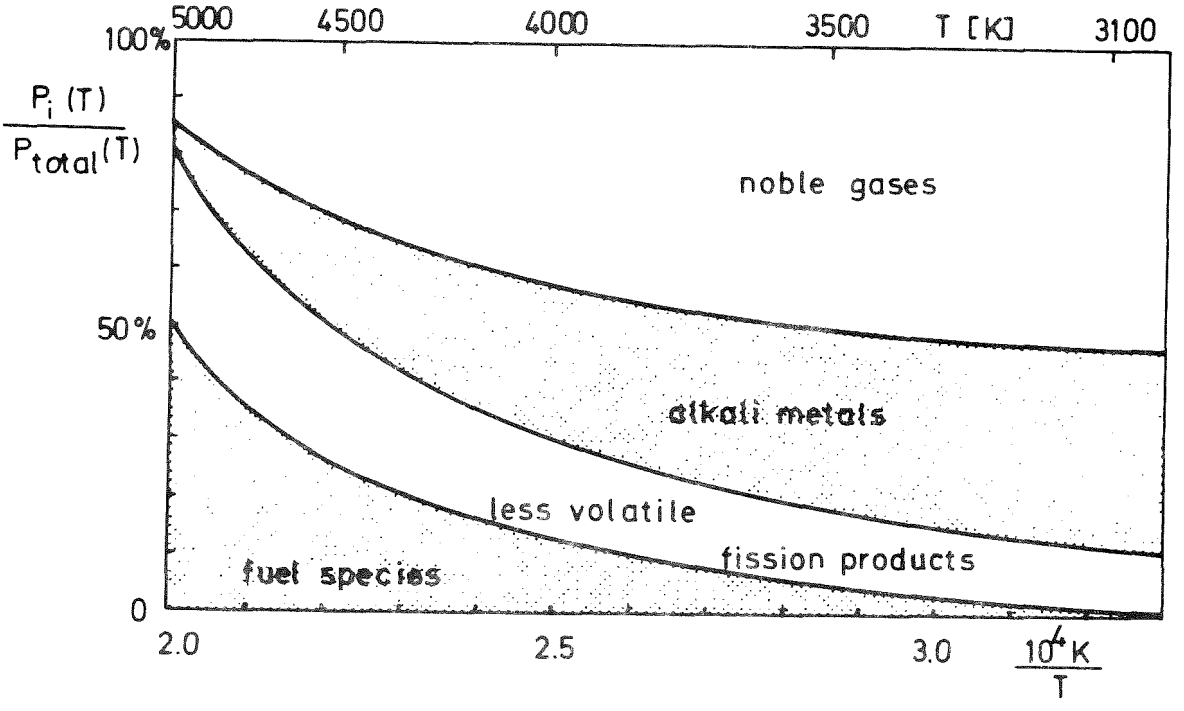

Fig.11 Contributions of fission products and fuel to the total vapor pressures.

5. EXPERIMENTAL APPROACHES TO THE PROBLEM OF GASEOUS PRESSURE DEVELOPMENT (EOS) OF IRRADIATED FUEL UP TO VERY HIGH TEMPERATURES

Safety analysis of fast reactors requires the knowledge of the gaseous pressure development of irradiated fuel as a function of enthalpy and temperature, respectively. Under this topic two temperature regions have to be considered, the solid phase region below the melting point of the fuel, which is related to normal and accidental fuel pin operation, and the liquid phase region of the fuel up to 5000 K, which is related to the conditions of hypothetical core disruptive accidents.

In the lower temperature scale, i.e. below the melting temperature of the fuel, it are the fission gases and the volatile fission products (Cs, Rb, J, ect.) which primarily contribute to the gaseous pressure in the fuel. The PVT-data of these elements, and also of Sodium, are known from measurements which have been extended up to the critical point and above [22-24].

In the high-temperature region far above the fuel melting temperature, the partial pressures of the less-volatile fission products and of the fuel material itself become important in the total vapor pressure because of their high heats of evaporation. The essentially contributing elements are Nd, Ru, Pd, Ce, Se, Tc, Ag [1]. They exist in the liquid fuel partly as metals (Ru, Pd, Se, Tc), partly as oxides (Nd, Ce).

In the lower temperature scale, the equilibrium pressure of the irradiated fuel can be quantitatively derived from thermodynamic equilibrium data of the pure materials. However, to describe the dynamic pressure development in the fuel pin, the redistribution of the fission products and the retention of the fission gases have to be considered. While the process of redistribution can be described quantitatively [13,15,25], the theoretical models of fission gas retention [26] have yet to be verified experimentally [27].

In the high temperature region, the direct measurement of the total pressure of irradiated fuel appears not to be feasible. To overcome this lack of direct experimental data, the total vapor pressure of the liquid

fuel must be derived theoretically. The condition is a sufficient knowledge of the chemical state of the fission product species in the liquid fuel and in the vapor phase, and the knowledge of the vapor pressure curves of the pure fuel material and of the most relevant fission product species. The required partial vapor pressures can also be determined from thermodynamic calculations [1,5], if a reliable set of the enthalpies of formation is available, and if the oxygen potential of the liquid fuel system is known [5].

Up to now, no vapor pressure measurements have been performed with the fission product substances of interest at temperatures between 3000 K and 5000 K. Measurements with metallic fission products could offer the best chance of success. Difficulties are to be expected, however, in performing evaporation experiments with oxide fission products, because presently there is still too less knowledge on their complex evaporation behavior at elevated temperatures [28].

For direct experimental determination of the caloric and thermal equations-of-state of the fuel and fission product materials above 3000 K there are in principle only a few suitable high-temperature measuring techniques.

For measuring p(H) data, exploding wire techniques with direct electrical pulse-heating of the material should be excluded. The evaluation of the vapor-liquid equilibrium pressure would be a formidable task. A successful experimental attempt for determination of p(H) could be another instationary measuring method which is based on pulse electron-beam heating of the sample in a quasy-closed system [29].

For measuring p(T) data above 3000 K, when also the vapor-liquid equilibrium temperature has to be measured, open-evaporation measuring methods appear to be more feasible. Electron-beam heating should not be applied because the interaction of the electron beam with the vapor cloud above the target would affect the evaporation velocity and the reaction pressure of the vapor cloud, and would also falsify the temperature measurement. Besides, the large penetration depth of the electron beam would cause an undefined explosion-like evaporation. Laser beam heating, however, offers a suitable heating technique for evaporation experiments up

to 5000 K. It allows quasi-stationary measurements of p(T) data based on determination of the stationary evaporation velocity of the target material and of the reaction pressure of the vapor [30].

With laser techniques, vapor pressure measurements at temperatures up to 5000 K have been performed up to now with pure oxide fuel materials [31-34] . The evaporation behavior of UO_2 and (U,Pu) mixed oxide is sufficiently known to allow reliable interpretation and evaluation of open evaporation experiments with liquid oxide fuel [35]. The required equilibrium vapor pressure curve can be derived from the measurements by use of Breitung's oxygen potential approach [5,36] . The measuring method and the evaluation model are shortly described in the following.

Fig.13 shows the measuring principle. A rectangular laser pulse of 1 to 10 ms pulse length, cut out from the continuous beam of a high-power CO_2 laser, is focused on the sample positioned in a vacuum chamber. The sample is locally heated to the liquid state up to temperatures of 5000 K. By a rotating wobble mirror, the laser focus, during the pulse, is uniformly moved on a circular trace on the specimen surface. (This procedure allows to evaporate relatively large amounts of liquid target material from a nearly flat surface area). The measuring quantities are:

- evaporation time and area,
- evaporated mass, measured by direct weighing of the mass of the collected vapor,
- forward momentum of the vapor jet, measured from the amplitude of the pendulum collector
- spectral thermal radiation of the evaporating surface, measured with a fast micropyrometer.

The vapor pressure of the target material is derived from the mechanical measuring quantities. The evaporation temperature in a first approach has been determined from the momentum of the vapor jet by use of a gas dynamic evaluation model of the fuel vapor expansion in the vacuum. In a second approach, in the temperature region below 4000 K, the evaporation temperature of the fuel sample has been determined pyrometrically. The condition was, however, to measure the spectral emissivities of the liquid fuel. For this reason, the spectral emissivities of UO_2 have been

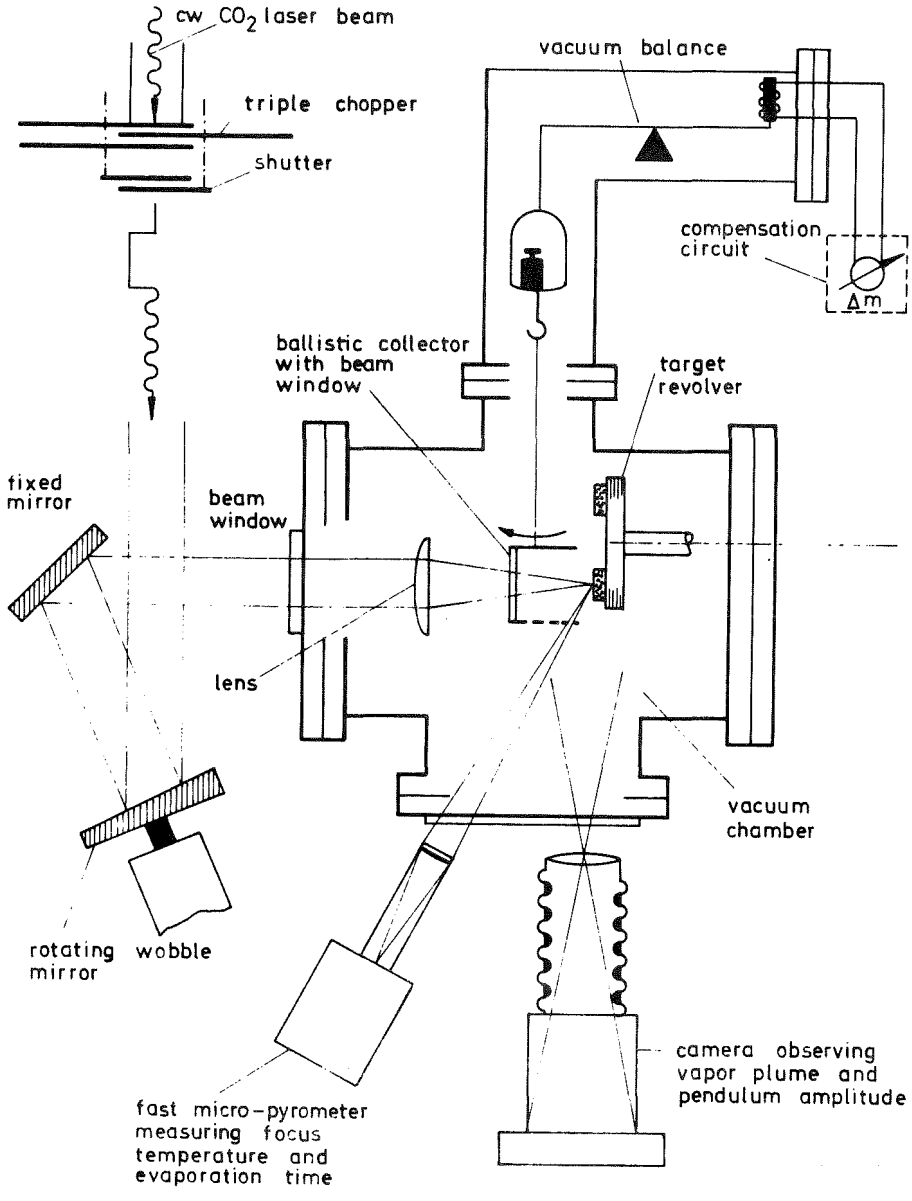

Fig.13 Measuring principle of laser evaporation experiments to determine the vapor pressure of oxide fuel up to 5000 K.

determined up to 4000 K with a laser integrating sphere reflectometer [37].

An application limit of these vapor pressure measuring techniques is given by onset of plasma interaction of the vapor plume with the incident laser beam at temperatures above 4500 K. Movement of liquid material in the laser crater caused by the reaction pressure of the vapor jet does not disturb such vapor pressure measurements where the measuring quantities are the evaporated mass or the reaction pressure of the vapor [32].

The application limits of pyrometry for measuring the evaporation temperature are given by two effects, interaction of the thermal radiation of the target surface with the fuel vapor cloud, and formation of too large temperature gradients in the evaporating fuel layer because of the intense surface evaporation cooling. Therefore, the pyrometric measurement of the evaporation temperature appears to be reliable up to temperatures around 4000 K.

Another important aspect arises from the fact, that the dynamic vapor pressure measurements on liquid oxide fuels with laser heating techniques imply strong alterations in the composition of the incongruently evaporating fuel surface [35]. During open evaporation, the depletion in the preferentially evaporating components cannot be restored by diffusion from the bulk material. After a short transient evaporation period stationary surface-evaporation is reached with a surface composition which differs greatly from the given fuel composition and depends on the actual evaporation temperature. When this stationary forced-congruent evaporation mode is reached, the gross vapor composition is well-defined and is identical to the bulk composition of the fuel which is quite different from the actual surface composition. In consequence, the total vapor pressure developing in open surface-evaporation of a liquid oxide fuel can substantially deviate from its thermodynamic equation-of-state, in the case of $(U_{0.80}Pu_{0.20})$ mixed oxide by a factor of 2 to 7 depending on the O/M-ratio (Fig.14). The required equation-of-state of liquid mixed oxide, however, can be deduced in a further step from the vapor pressure curve measured in open evaporation by the thermodynamic model of Breitung [5,36] .

Experimental values for the saturated vapor pressure of UO_2 are presented in Fig.15, determined from five series of laser evaporation measurements obtained at temperatures between 3500 K and 4200 K. For comparison, the vapor pressure curve for forced congruent evaporation of $UO_{2.00}$ is shown, calculated by Breitung, which relates to the open evaporation of UO_2. There is fairly good agreement of this thermodynamically derived curve with the laser vapor pressure measurements reported above.

This short review on the experimental approaches to measure p(T)-data for fast reactor safety analysis shows that the laser evaporation method turns out to be a suitable measuring method. The next step should be to extend the measurements to the fission product materials which

essentially contribute to the pressure development of irradiated fuel. This requires an extension also of the theoretical and experimental studies on the chemical and kinetic evaporation behavior of these substances.

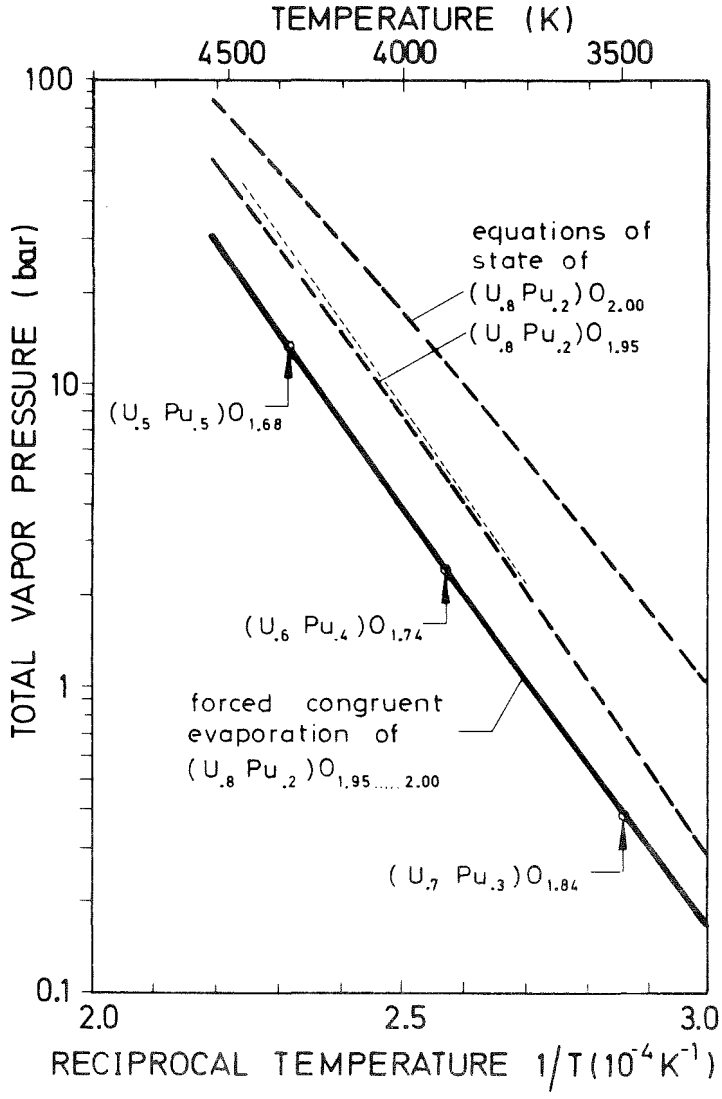

Fig. 14 Theoretical vapor pressure curves of Breitung for liquid-vapor equilibrium (equations-of-state) of $(U_{.8}Pu_{.2})O_{2.00}$ and $(U_{.8}Pu_{.2}O_{1.95}$, and for open evaporation (forced congruent evaporation) of $(U_{.8}Pu_{.2})O_{1.95...2.00}$! Along the latter curve, the fuel surface compositions are given which actually exist at different temperatures during open evaporation of $(U_{.8}Pu_{.2})O_{1.95...2.00}$. The dotted line represents the vapor pressure curve recommended by Ohse.

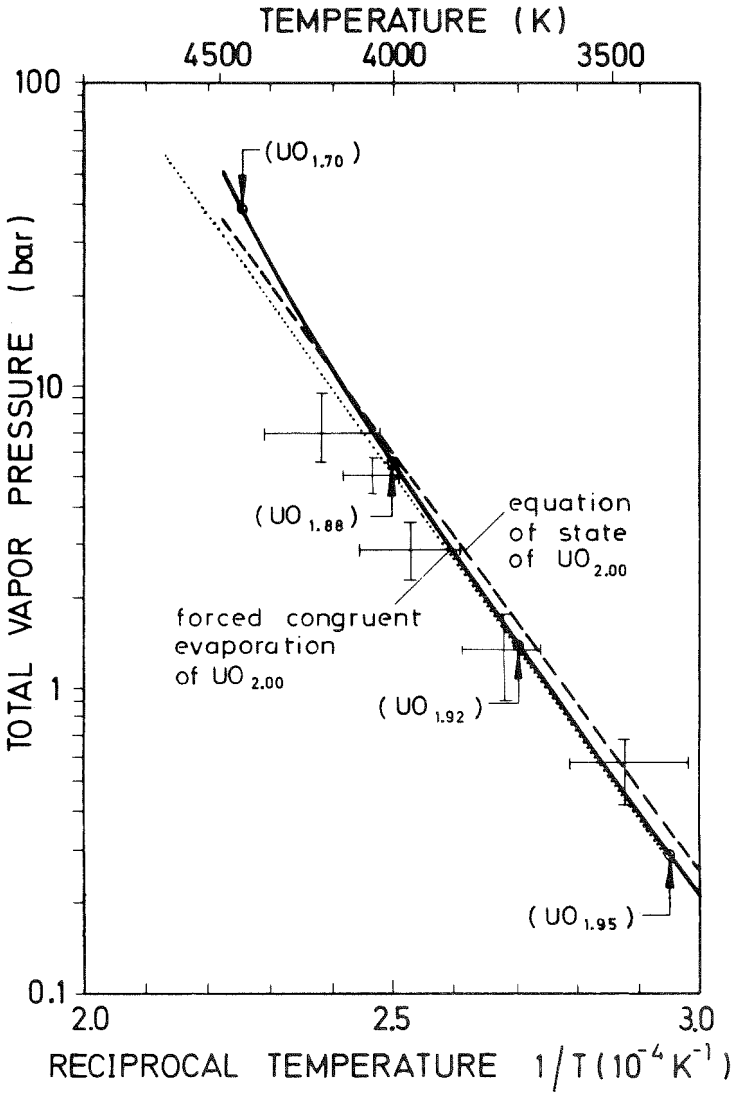

Fig. 15 Theoretical vapor pressure curves of Breitung for liquid-vapor equilibrium (equations-of-state) of $UO_{2.00}$, and for open evaporation (forced congruent evaporation) of UO_2. Along the latter curve, the fuel surface compositions are given which actually exist at different temperatures during open evaporation of UO_2. The cross marks represent the vapor pressure of open evaporating UO_2 directly measured with the above described laser evaporation method. The dotted line represents the vapor pressure curve recommended by Ohse.

6. THEORETICAL STUDIES ON THE THERMODYNAMIC STATE AND GAS KINETIC BEHAVIOR OF FUEL VAPOR AT VERY-HIGH TEMPERATURES

The conditions for nuclear reactor safety analysis include the knowledge of the caloric and thermal equations-of-state, i.e. H(T) and P(VT), of the liquid phase and of the liquid-vapor equilibrium of the irradiated fuel up to temperatures of about 5000 K. Besides the thermodynamic functions-of-state, the heat and radiation transport properties of the saturated fuel vapor are of interest. Knowledge is also needed on the relaxational and gas dynamic behavior of adiabatically expanding fuel vapor. In this context, the problem arises of cluster and aerosol formation during open evaporation of liquid fuel under accident conditions.

In a first theoretical approach, the thermodynamic equilibrium state of saturated fuel vapor over liquid UO_2 has been investigated, including an evaluation of the plasma state of the partly ionized fuel vapor. The caloric functions-of-state, H(T) and C(T), of saturated UO_2 vapor have been deduced up to 5000 K by means of statistical mechanics from the multicomponent molecular structure and from the kinetic and plasma state of the fuel vapor [38]. For comparison, enthalpy data also of the condensed phases of UO_2 have been used to calculate vapor phase data.

In addition, the gas kinetic relaxation and flow structure of adiabatically expanding (laser-generated) UO_2 vapor jets have been considered. A better understanding of the gas dynamic phenomena and of the sheath boundary effects eventually occuring during intense surface evaporation of liquid oxide fuel would also allow a better interpretation and evaluation of laser evaporation experiments carried out with fuel.

The gaseous and plasma state of UO_2 vapor at temperatures between the UO_2 melting point (3130 K) and 5000 K is quantitatively characterized in Table 3. It describes the gas kinetic state of oxide fuel vapor consisting of UO_2 or 'UO_2-like' molecules, ions and free electrons. The temperature and total vapor pressure data p(T) given in the two first columns are based on laser vapor pressure measurements [30,32,35] and on the theoretical evaluation of the UO_2 vapor pressure curve by Breitung [5,35] . The

T/K kT/eV	p bar	n_{tot} cm^{-3}	d_o Å	χ_i %	n_q cm^{-3}	d_q Å	l_D Å	l_L Å	λ_e Å	N_D	q_{LD}	λ_{PL} µm	E_i^{pl} eV	v liter/mole	A	ρ mg/cm³
3130 .270	.075	1.74 E17	111	.67	1.16 E15	590	800	53	24	1	.1	1000	5.0	3470	a)270 b)269 c)267	.08
3600 .310	1	1.97 ·E18	49	1.2	2.36 ·E16	210	190	46	22	∿.3	.3	220	4.7	306	a)270 b)269 c)265	.88 .88 ·87
4000 .345	5	8.89 ·E18	30	1.8	1.60 ·E17	110	77	42	21	∿.07	.6	80	4.5	68	a)270 b)268 c)263	3.97 3.94 3.86
4400 .379	20	3.23 ·E19	19	2.7	.872 ·E18	100	35	38	20	∿.04	1.1	36	4.2	18.9	a)270 b)266 c)259	143 14.0 13.7
5000 .431	100	1.45 ·E20	12	∿5	7.2 ·E18	30	13	33	19	∿.02	2.5	12	3.7	4.15	a)270 b)262 c)250	65 63 60

Table 3 Characteristic data describing the gas kinetic and plasma state of UO_2 vapor between 3100 K and 5000 K.

calculation of the degrees of ionization, χ_i, of oxide fuel vapor with the Saha equation does not work right off because the effective ionization energy E_i^{pl} of a vapor molecule differs remarkably from the theoretical value of the isolated molecule under the actual vapor conditions above 3000 K. The different effects which lower the ionization energy partly in an additive manner are discussed in detail in Ref. [38].

As can be seen from Table.3, oxide fuel vapor in the temperature range from the boiling point up to 5000 K represents both a dense gaseous system and a strong plasma. The neutral vapor component behaves up to 5000 K as a perfect gas. This can be seen from an estimation of the van-der-Waals constants of UO_2 vapor. The ionized component of the fuel vapor, however, does not approach to the state of a perfect kinetic plasma. At temperatures around 5000 K, UO_2 vapor represents a so called classical collective plasma [38] with increasingly "metallic" properties elucidated

by the fact that at temperatures between 4500 K and 5500 K the de Broglie wavelength λ_e of the free plasma electrons should reach the magnitude of the mean particle distance d_o and d_q, respectively. There is than no more a kinetic but a wave mechnical interaction of the elctron gas with the neutral and ionized molecules in the UO_2 vapor.

Saturated vapor over liquid UO_2 consists not only of UO_2 molecules but to a remarkable extent also of UO_3 and UO molecules, and of monatomic oxygen. For the temperature range far above 3000 K no experimental data exist on the vapor composition. However, detailed thermodynamic calculations on the equilibrium partial pressures over liquid oxide fuels up to 5000 K have been performed by Breitung [5]. From this numerical set of partial pressures the molecular composition and the average atomic weight of the vapor can be derived. The results are given in Table 3 . The effect of the electron gas to the average atomic weight of the fuel vapor has been simply estimated using the ideal gas law.

The nonuniform vapor composition underscores the fact that saturated vapor of liquid UO_2 consists of chemically reactive molecular species. The total oxygen content in the vapor is higher than in the liquid phase as is shown by the superstoichiometric O/U-ratio of the vapor. Also the average number of oxygen bonds per vapor molecule, $\bar{\nu}$, is larger than in the liquid UO_2 phase - indicating oxidation reactions taking place during the evaporation process. On the other hand, $\bar{\nu}$ is smaller than the O/U-ratio of the vapor - indicating onset of dissociative reactions with increasing temperature. Quantitative results are given in Ref. [38].

The caloric functions-of-state of saturated UO_2 vapor, especially the functions of enthalpy and specific heat, have been derived by means of statistical mechanics. By use of spectroscopic molecular data of the vapor molecules, the vibrational and rotational energy contributions of the vapor molecules can be calculated straight forward.

No experimental data, however, exist on the electronic states of the neutral or ionized uranium oxide molecules. Therefore, a more general approach has been taken to generate the electronic partition function of UO_2, which is not restricted to a molecule of ionic bond type. The energy spectrum of the unoccupied electronic states of a polyatomic molecule can

be represented by a Rydberg series of states. In reality, this discrete energy spectrum has to be replaced by a smeared, continuum-like spectrum, because there is no energy degeneracy of the Rydberg states in a strongly bound polyatomic molecule. Furthermore, the line broadening and splitting by impacts and Stark effect of a molecule immersed in dense and partly ionized UO_2 vapor smear the partition function. These considerations lead to a fairly simple calculational approach for estimation of the internal energy of the electronic states [38]. The results show that their contribution corresponds to about 2 to 2.4 thermal degrees of freedom between 3100 K and 5000.

Summing up the contributions of all molecular degrees of freedom yields the total enthalpy function of saturated vapor over liquid UO_2 (Fig.16). Zero reference state is related to the gaseous elements U and

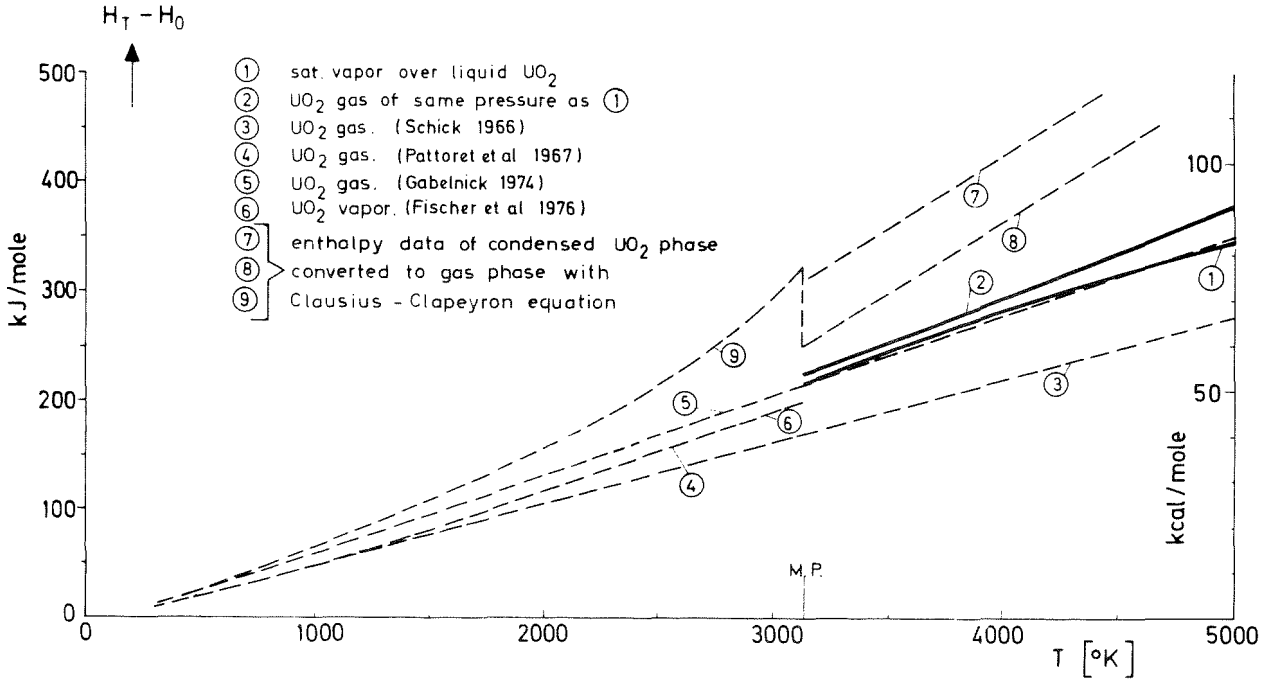

Fig.16 Enthalpy function $H^o(T)-H^o_0$ of
1) saturated UO_2 vapor of equilibrium composition
2) 'pure UO_2 gas', assuming monocomponent vapor composition of UO_2 molecules

0 at 0 K. The vapor composition is assumed to be the same at temperature T and reference temperature T_o. Derivation at constant vapor composition yields the specific heat function $C_p(T)$ which is shown in Fig.17. For comparison, the figures contain also the enthalpy and specific heat function calculated for "pure UO_2 gas", i.e., assuming vapor composition of UO_2 molecules only (curves No.2).

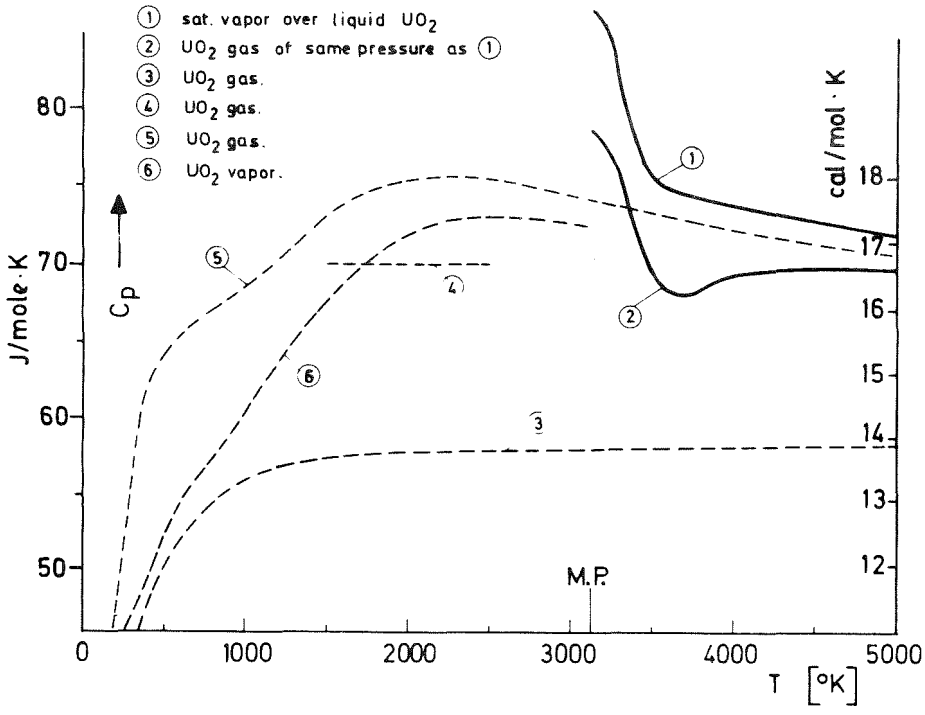

Fig.17 Specific heat $C_p(T)$ of
1) saturated UO_2 vapor of equilibrium composition
2) 'pure UO_2 gas'

The non-monotonous slope with temperature of the new specific heat functions is primarily caused by the changes in the vapor composition and in the plasma state with temperature. The overshoot of $C_p(T)$ near the melting point of UO_2 (3130 K) is caused by the onset of thermal excitation of the electronic states, and of thermal ionization of the vapor molecule. At temperatures up to 5000 K, the relative contribution to the enthalpy from the plasma state turns out to be small. The negative binding energy of the plasma still diminishes its role in the energy balance of UO_2 vapor. However, the dense plasma state of UO_2 vapor could significantly stamp its optical and radiation properties and eventually influence the liquid-vapor equilibrium.

The determination above of the enthalpy and specific heat functions of high-temperature UO_2 vapor differs partly from previously published approaches because it comprises the plasma state of saturated UO_2 vapor

and the thermal excitation of electronic states. In addition the temperature dependent equilibrium composition of uranium oxide vapor over liquid UO_2 has been taken into account. For these reasons deviations of previously published thermodynamic UO_2 vapor functions from the approach presented here appear to be reasonable.

It would be interesting to compare, if possible, the present enthalpy data of gaseous UO_2 with enthalpy data from literature of the condensed UO_2 phases. For that purpose, the enthalpy data set of solid and liquid UO_2 recommended by Leibowitz et al. [40] is converted to the gaseous phase tentatively by means of the Clausius-Clapeyron equation for a monocomponent system. The enthalpy curves No.7 to 9 (Fig.16) represent the enthalpy conversion calculated with different heats of evaporation derived from Breitung's oxygen potential approach [5] and from the ANL data set [40], respectively. As the figure shows, the Clausius-Clapeyron approach yields very high enthalpy curves with too high slope, i.e., with too high specific heat functions of the vapor. The descrepancy should be caused by the application of the Clausius-Clapeyron equation to the UO_2 system.

Actually, application of the Clausius-Clapeyron equation tacitly assumes that the vapor-liquid equilibrium observed belongs to a single-component, chemically inert thermodynamic system. The oxide fuel system does not satisfy this assumption. Even restriction to the 'condensed UO_2 phase - gaseous UO_2 vapor component' partial system would not allow application of this equation because the partial system would not represent a closed thermodynamic system. For the same reasons, also results obtained from the generalized Clapeyron equation for multicomponent systems should also be viewed with reservation, if applied to the vapor-liquid equilibrium of oxide fuel system. - With the considerations above, the discrepancies of the enthalpy data in Fig.16 seem to be elucidated.

The approach above of calculating the caloric functions of the uranium oxide vapor species can be completed by determination of the free energy functions, including thermal ionization and electronic excitation. By use of Breitung's oxygen potential approach for the UO_2 system, this independent set of input data for the vapor phase together with appropriate data for the condensed phase would allow to verify the previously published curves of the equilibrium vapor pressure over liquid oxide fuel [5, 35, 36]

The relaxation kinetics and gas dynamic behavior of the oxide fuel vapor should be known to allow interpretation of the laser evaporation experiments and vapor pressure measurements recently carried out with oxide fuel. Knowledge of the kinetic and dynamic behavior of freely expanding oxide fuel vapor would also allow better modeling of the fuel pin failure mechanisms in fast reactor safety analysis. In this context, also the question of aerosol formation during open evaporation of liquid fuel needs to be cleared.

The kinetic state of a UO_2 vapor cloud, (laser-) generated by open surface evaporation of liquid UO_2, is highly collision-dominated. This involves a strong reaction of the flowing-off vapor on the evaporating surface. The intensive back-scattering from the vapor layer to the adjacent liquid surface lowers the evaporation velocity and eventually affects the evaporation coefficients of the vapor species. The collision-dominated state of the UO_2 vapor plume also involves an intensive kinetic interaction of the vapor particles leading to a gas dynamic vapor flow-off [30].

The enthalpy balance and the flow structure of the laser-generated UO_2 vapor jet is governed by kinetic relaxation during the adiabatic expansion into the vacuum. Tab.4 gives a first estimation of the relaxation channels and relaxation rates calculated for an evaporation temperature of 4400 K. At these temperatures, the enthalpy content of the vapor corresponds to about 17 thermodynamic degrees of freedom. Regarding the laser evaporation crater as a "sonic gas orifice", it can be derived from the experimental results, that only f_{rel} ~5 thermal degrees of freedom take part in the relaxation and are converted into kinetic flow energy of the vapor. This result looks reasonable, as is illustrated by Tab.4. It also shows that the electron gas effectively undergoes relaxation only with ~5 degrees of freedom of the heavy particles in inelastic collisions. Since the relaxation of energy is very ineffective in elastic collisions of the hot electron gas with the heavy UO_2 vapor molecules, this causes a "run-away effect" of the electrons during a fast vapor expansion. These estimations show, that local thermodynamic equilibrium is not attained in the vapor during fast expansion in open surface evaporation of liquid oxide fuel; this means, that the concept of 'thermodynamic temperature' can be hardly applied to the case of fast expanding fuel vapor.

At higher temperatures, at ~4500...5000 K, the real gas properties of the UO_2 vapor must be taken into account in the analysis of the adiabatic expansion. While at the lower temperatures the vapor expansion can be treated as isentropic, the Joule-Thomson effect can no more be neglected at these high temperatures. This isenthalpic, non-isentropic would cause a cooling effect of $\Delta T \sim -100$ K.

enthalpy transfer during relaxation of	degrees of freedom RT/2	transferred by relaxation collisions to kinetic energy of	
		vapor molecules	plasma electrons
molecular translation	3	x	(x)
rotational excitation	2	x	(x)
vibrational excitation	8		(x)
electronic excitation	∿ 2.5		x
dissociation-recombination	∿ 2		x
ionization-recombination	∿ 1		x
cluster formation	∿ .5	x	(x?)

Table 4 Enthalpy balance and relaxation channels of freely expanding UO_2 vapor jets at 4400 K.

Table 4 contains a first estimation of the energy release caused by cluster formation in freely expanding UO_2 vapor. The generation of clusters is to be expected, because the adiabatic expansion of the UO_2 gas is starting very near the saturated vapor pressure curve passing instantaniously over into the supersaturated region. This mean ideal conditions for clustering. However, because of the low molecular collision number during the whole expansion, the cluster size should, on an average, only be about 50 molecules per cluster molecule - corresponding to a cluster size of about 20 Å. This theoretical prediction which is based on experimental studies carried out by Obert [41] on cluster formation of different vapor species, agrees with our experimental result, according to which no condensation of uranium oxide cluster molecules could be detected in laser evaporation experiments using an electron microscope of ≥ 20 Å-resolution [30].

The degree of cluster formation should be a few per cent of the vapor molecules. In this estimation it was not even taken into account that cluster formation in oxide fuel vapor should not be limited by spontaneous nucleation. The high particle density of ionized vapor molecules, which represent ideal condensation nuclei, could enhance the rate of clustering. The present state of theories on condensation in neutral and partly ionized vapor is still rather incomplete so that more accurate estimates cannot yet be made on cluster formation in oxide fuel vapor. It is planned, therefore, to approach this problem by laser evaporation experiments. For this purpose, a special retarding-field cluster detector will be used.

A final remark should be added concerning the assumption of local thermodynamic equilibrium which exists at the boundary between the evaporation liquid surface and the vapor plume. This assumption should not be regarded as a natural fact because of the dense plasma state of oxide fuel vapor above 3000 K. The liquid fuel surface should also be considered as a highly intensive thermionic emitter, being in thermal contact with a very dense plasma. Then, plasma physics predicts the eventual existence of a non-neutral plasma boundary sheath separating the electrically neutral vapor plume from the liquid UO_2 surface. Such a boundary sheath would then cause, e.g., an electrical field strength of about 0.6 10^6 V/cm normal to a liquid UO_2 surface being at 4000 K. This could influence the evaporation process and the evaporation coefficients of the vapor species.

In this approach to the thermodynamic state of oxide fuel vapor, the vapor-liquid equilibrium of pure UO_2 fuel system has been considered. To extend the approach to burnt-up fuel systems, the alterations of results have to be studied which occur when typical fission product species are added to non-irradiated fuel. In this procedure it should be taken into account that a burnt-up fuel system cannot be expected to reach total thermodynamic equilibrium of all its components in the liquid and gaseous phase under pin meltdown or core disruptive accident conditions. Otherwise, one could overestimate, e.g., the influence of the alkali metal fission product species on the plasma state and on the total pressure of the gaseous phase of the fuel.

LITERATURE

[1] S.D.Gabelnick, M.G.Chasanov
A calculational approach to the estimation of fuel and fission-product vapor pressures and oxidation states to 6000 K,
ANL-7867, (Oct. 1972).

[2] M.H.Rand, T.L.Markin
Some Aspects of $(U,Pu)O_2$ solid solutions and their use as nuclear fuels,
in "Thermodynamics of Nuclear Materials", p.637, IAEA Vienna (1967).

[3] M.Tetenbaum
High temperature vaporization behavior of hypostoichiometric U-Pu-O and U-Nd-O solid solutions,
in "Thermodynamics of Nuclear Materials", p.305, IAEA, Vienna (1975).

[4] W.Breitung
Berechnung des Sauerstoffpotentials von $(U,Pu)O_{2\pm x}$ mittels Defektmodellen und gemessener Daten im Temperaturbereich von 1000-1700 K,
KFK-2363 (Oct.1976).

[5] W.Breitung
Berechnung der Dampfdrücke von oxidischen Brennstoffen bis 5000 K bei Gleichgewichts- und Nichtgleichgewichtsverdampfung,
KFK-2091 (Juni 1975).

[6] T.L.Markin, E.J.McIver
in "Plutonium 1965", London Chapman a, Hall, P.845 (1967).

[7] F.Schmitz
Electrical conductivity of $(U,Pu)O_{2\pm x}$ in the pure state and with addition of Mo,
in "Plutonium 1975 and other actinides" Amsterdam, North Holland Publ.Co., p.171 (1976).

[8] R.F.Woodley
Equilibrium oxygen potential-composition relations in $(U_{0.75}Pu_{0.25})U_{2-x}$,
J.Am.Cer.Soc. 56, 3, 116 (1973).

[9] P.E.Blackburn, C.E.Johnson
"Chemical modelling of uranium plutonium and oxygen redistribution in oxide fuels...",
in "Thermodynamics of Nuclear Materials, p.17, IAEA Vienna (1975).

[10] M.de Franco, J.P.Gatesoupe
The thermodynamic properties of $(U,Pu)O_{2\pm x}$ described by a cluster model,
in "Plutonium 1975 and other actinides", Amsterdam, North Holland Publ.Co., (1976) p.133.

[11] C.Sari, G.Schumacher
Oxygen transport in fast reactor oxide fuel,
Journ.Nucl.Mater. 61, 192 (1976).

[12] H.Kleykamp
Die radiale Sauerstoffverteilung im Brennstoff bestrahlter Mischoxid-Brennstäbe unterschiedlicher Ausgangsstöchiometrie,
Journ.Nucl.Mater. 66, 292 (1977).

[13] M.Bober, G.Schumacher
Material transport in the temperature gradient of fast reactor fuels
in "Advances of Nuclear Science and Technology", Vol.7, Academic Press New York (1973).

[14] H.Kleykamp
Formation of phases and distribution of fission products in an oxide fuel,
in "Behavior and chemical state of irradiated ceramic fuels IAEA-Vienna, p-157 (1974).

[15] H.Kleykamp
in "UO_2-PuO_2-Brennstabbündel-Bestrahlung DFR-350",
KFK-1960 p.29 (1974).

[16] P.D'Annucci, C.Sari, G.Schumacher
Migration of metallic fission products in reactor oxides fuels,
J.Nucl.Technology, in print.

[17] M.Bober, G.Schumacher
Erhöhung der Zentraltemperatur durch Uran-Plutonium-Entmischung
in Mischoxid-Brennstäben schneller Reaktoren,
KFK-1904 (1974).

[18] M.G.Adamson
Out-of-pile experiments performed in the U.S. FCCI program in
Summary Report of the IAEA International working group on fast reactors
Technical Commitee Meeting on fuel and cladding interactions,
Tokyo, Japan, Febr. 21-25, 1977.

[19] F.Schmitz
Potential d'oxygene et structure de defaut de l'oxyde mixte $(U,Pu)O_{2-x}$,
Journ.Nucl.Mater. 58 (1975) 357.

[20] T.L.Markin, E.C.Crouch
Thermodynamic data for U-Ce-oxides,
J.Inorg.Nucl.Chem. 32 (1970) 77.

[21] O.T.Sorensen
Thermogravimetrie studies of the high temperature thermodynamic
properties of nonstoichiometric cesium oxides,
Proceedings of the 3.International, Conf. on Thermal Analysis Davos,
1971, Wiedemann Editor.

[22] Yu.S.Korshunov, S.P.Vetchinin, A.P.Senchenkov, E.I.Asinovski
Certain Thermodynamic Properties of Cesium at High Temperatures
and Pressures,
Teplofiska Vysokih Temperatur Vol.13 (1975) 517-525.

[23] I.L.Silver, C.F.Bonilla
The High Temperature Vapor Pressure and the Critical Pressure and Temperature of Cesium by Direct Measurement,
Proc. 5th Symposium on Thermophysical Properties, Am.Soc.of Mech.Eng. New York, 1970, p.461-467.

[24] V.S.Bhise, C.F.Bonilla
The Critical and High Temperature Equilibrium Phase Densities of Sodium and Potassium,
Proc. of the 7th Symposium on Thermophysical Properties, National Bureau of Standards, Washington D.C., 1977, in print.

[25] G.de Contenson, J.Monier, N.Vignesoult
Distribution des Produits de Fission et Localisation par Spectrometrie Gamma en cours d'Irradiation et après Irradiation,
Proc. IAEA Panel on the Behavior and Chemical State of Irradiated Ceramic fuels, Vienna 1974, p.191.

[26] C.Ronchi, Hj.Matzke
Calculations and Estimates of the Contributions of Different Transport Mechanisms to the Fission Gas Behavior in Fast Breeder Oxide Fuel,
Proc. on the IAEA Symp. on Fuel and Fuel Elements for Fast Reactor 1973, Vienna 1974.

[27] J.R.Findley eta 1.
Fast Reactor Safety Studies Using VIPER,
Proc. US-Japan-Seminar on Fast Pulse Reactors, Jan 1976.

[28] M.Tetenbaum
Some Aspects of the High Temperature Vaporization Behavior and Valence Effects in Actinide-Oxide Rare-Earth-Oxide Systems,
Int.Collog. on Refractory Oxides for High Temperature Energy Sources, Odeillo, France 1977.

[29] D.A.Benson, W.H.Buckalew.
The Uranium Dioxide Vapor Equation-of-State,
Trans. ANS 23 (1976) 325.

[30] M.Bober, H.U.Karow, K.Schretzmann
Evaporation Experiments to Determine the Vapor Pressure of UO_2 Fuel (3000-5000 K),
Proc.IAEA Symp. om Thermodynamics of Nuclear Materials 1974, Vol.1, p.295, Vienna 1975.

[31] M.Bober, H.U.Karow, K.Schretzmann
Vapor Pressure Measurements of Oxide Fuel Between 3000 and 5000 K Using Laser Heating,
Nuclear Technology 26 (1975) 237.

[32] M.Bober, W.Breitung, H.U.Karow, K.Schretzmann
Evaporation Studies of Liquid Oxide Fuel at Very High Temperatures Using Laser Beam Heating,
(Gordon Research Conf. on High-Temperature Chemistry, Tilton, N.H., (1976), Report KFK-2366 (1976).

[33] R.W.Ohse, P.G.Berrie, G.D.Brumme, P.R.Kinsman
Advances in Vapour Pressure Studies Over Liquid Uranium Plutonium Oxides up to 5000 K,
Proc. 5th Conf. Plutonium and other actinides 1975, Baden-Baden, Vol.1, North-Holland Publ.Comp., Amsterdam, 1976, p.191.

[34] J.F.Babelot, G.D.Brumme, P.R.Kinsman, R.W.Ohse
Vapour Pressure Measurements Over Liquid UO_2 and $(U,Pu)O_2$ by Laser Surface Heating up to 5000 K,
Proc. Reaktortagung Mannheim 1977, p 351.

[35] M.Bober, W.Breitung, H.U.Karow, K.Schretzmann
On the Interpretation of Vapor Pressure Measurements on Oxide Fuel at Very-High Temperatures for Fast Reactor Safety Analysis
Journal Nucl.Mater. 60 (1976) 20.

[36] W.Breitung
Verdampfungskinetik von oxidischen Kernbrennstoffen und ihr Einfluß auf die Spaltstoffentmischung in Reaktorbrennstäben und auf den Brennstoffdampfdruck unter Störfallbedingungen,
Report KFK-2240 (1976).

[37] M.Bober, H.U.Karow.
Measurements of Spectral Emissivity of UO_2 Above the Melting Point
Proc. of the 7th Symposium on Thermophysical Properties, National Bureau of Standards, Washington D.C., 1977, in print.

[38] H.U.Karow
Thermodynamic State, Specific Heat, and Enthalpy Function of Saturated UO_2 Vapor between 3000 K and 5000 K",
Report KFK-2390 (1977), and Proc. 7th Sympo. on Thermophysical Properties, National Burau of Standards, Washington D.C., 1977, in print.

[39] L.Brewer, and G.M.Rosenblatt
Dissoziation Energies of Gaseous Metal Dioxides,
Chem.Rev.61, 1961, 257-263.

[40] L.Leibowitz, (Ed.)
Properties for LMFBR Safety Analysis,
Report ANL-CEN-RSD-76-1 (1976).

[41] W.Obert
private communication.